ABSTRACT

Title of Thesis:	Self-assembled synthetic polymer complexes for delivery of immunomodulatory nucleic acids
	Neil Martin Dold, Master of Science, 2017
Thesis Directed By:	Associate Professor, Christopher M. Jewell, Fischell Department of Bioengineering

Biomaterials that provide precision control over immune function could enable next generation vaccines and immunotherapies for infectious diseases, cancer, and autoimmune diseases. Rational design of biomaterial delivery vehicles allows use of conventional benefits of drug delivery vehicles – for example co-delivery, controlled release, and targeting – and newly discovered immunomodulatory effects that arise from the physicochemical features of delivery vehicles. This thesis investigates the intrinsic ability of poly(ß-amino esters) to stimulate immune cells in both soluble and nanoparticle form. Further, it examines the intrinsic stimulatory capacity of rationally designed self-assembled RNA nanostructures delivered to immune cells in soluble form and when complexed with poly(ß-amino esters) to enhance immune stimulation. These studies take advantage of two models of innate immunity using primary mouse dendritic cells and a macrophage cell line to characterize immune response. Knowledge linking physicochemical features of these formulations to inflammatory mechanisms could support more rational design approaches for vaccines and immunotherapies.

SELF-ASSEMBLED SYNTHETIC POLYMER COMPLEXES FOR DELIVERY OF IMMUNOMODULATORY NUCLEIC ACIDS

by

Neil Martin Dold

Thesis submitted to the Faculty of the Graduate School of the
University of Maryland, College Park, in partial fulfillment
of the requirements for the degree of
Master of Science
2017

Advisory Committee:
Professor Christopher Jewell, Chair
Professor Kimberly Stroka
Dr. Bruce Shapiro

Acknowledgements

First and foremost, I would like to thank Chris and the members of the Jewell Lab for their guidance and help over the past several years. I would also like to thank Dr. Bruce Shapiro and his team for their collaborative efforts, with special thanks to Lorena for her dedication and enthusiasm over the past year. Finally, I thank my classmates, family, and friends who have supported me throughout my graduate education.

Table of Contents

List of Tables

List of Figures

List of Abbreviations

APC	Antigen presenting cell
CTLA-4	Cytotoxic T-lymphocyte-associated protein 4
DC	Dendritic cell
DLS	Dynamic light scattering
DsiRNA	Dicer-substrate small interfering RNA
ELS	Electrophoretic light scattering
IL-#	Interleukin-#
IRF	Interferon regulatory factor
LPS	Lipopolysaccharide
NC1	Control DsiRNA sequence
NF-κB	Nuclear factor kappa-light-chain-enhancer of activated B cells
NP	Nanoparticle
OVA	Ovalbumin
PBAE	Poly(ß-amino ester)
PD-1	Programmed cell death protein 1
RNA NS	RNA nanostructure
RNAi	RNA interference
siRNA	Small interfering RNA
TIM-3	T-cell immunoglobulin and mucin-domain containing-3
TLR	Toll-like receptor
TLRa	Toll-like receptor agonist

Chapter 1 : Scope and Organization

The immune system is a central player in human health, and its reach goes far beyond protecting us from infectious disease. Immune function can become dysregulated, causing autoimmune disorders like multiple sclerosis and type 1 diabetes, and it can support biological conditions that permit cancer to thrive. Fortunately, medical interventions through immunotherapies and vaccines provide promise in combating these dysregulated states, and many of the pharmaceutical industry's best-sellers directly target immune pathways. Yet, despite significant progress in this area, we have yet to see a significant number of clinical treatments that take advantage of biomaterial delivery vehicles: technologies that offer co-delivery, controlled release, and targeting. These biomaterials could provide precision control over interactions with the immune system, supporting public health benefits in efficacy, robustness across patient populations, and patient compliance. Moreover, biomaterials provide new opportunities for formulating treatments for autoimmune diseases and cancers where more traditional approaches have not achieved desired efficacy.

One of the emerging challenges in this space involves the effects of individual biomaterial carriers on the immune system, including those that result from the physicochemical features of important synthetic polymers. For example, recent studies reveal that particles widely used in the field of controlled drug release can initiate inflammatory responses when engulfed by immune cells. Work in our lab has shown that activation of immune cells may depend on a polymer's molecular weight, degradation, and form of delivery (i.e. particulate or soluble). To rationally design

vaccines and therapeutics with biomaterials to elicit desired immune responses, we need to understand how these materials modulate immune function. This thesis centers on self-assembly platforms combining degradable synthetic polymers and nucleic acids in self-assembled nanoparticle complexes. The studies elucidate how features of these complexes – which mimic a common vaccination and immunotherapy scheme based on nucleic acid condensation – elicit responses in immune cell lines and primary immune cells. In particular, the work focuses on the pro-inflammatory response induced by the platform in common primary and immortalized antigen presenting cells (APCs) derived from mice. These efforts were untaken in two aims:

1. Characterization of the intrinsic immunogenicity of a poly(ß-amino ester) (PBAE) in soluble and complexed form as a delivery vehicle for DNA encoding antigens or RNA interfering (RNAi) with immune pathways and
2. Investigation of the intrinsic immunogenicity of rationally designed RNA nanostructures (RNA NS) – rings and cubes, for example – in soluble and PBAE complexes for use as pro-inflammatory signals.

To carry out the aims, characterization of immune responses elicited by polymer and nucleic acid components were assessed *in vitro* using the RAW264.7 immortalized mouse macrophage cell line and in primary dendritic cells (DCs) isolated from mice. Other major components of the investigation included characterization of 1) physiochemical properties of complexes formulated with PBAE and dicer-substrate small interfering RNAs (DsiRNAs) or RNA NS and 2) potential immune pathways responsible for intrinsic immunogenicity. In each case, the RNAs selected do not target

immune cell function via RNA interference, but certain forms are able to activate immune pathways, likely by triggering immune danger signals.

In **Chapter 2**, a broad survey provides context for the use of biomaterials in controlling immune function, ending with more specific background in the area of self-assembled materials for vaccines and immunotherapies. Complex characterization and immune response elicited by soluble or complexed PBAE and DsiRNA is first described in RAW264.7 cells in **Chapter 3**, while **Chapter 4** describes immune activity in both immortalized and primary APCs using RNA displaying designed nanostructural shapes in soluble and complexed form. Both **Chapter 3** and **Chapter 4** discuss specific ongoing and future directions for elucidating the mechanisms responsible for immune stimulation.

Chapter 2 : Engineering materials to control the immune system[†]

2.1 Introduction

The traditional view of vaccines is one of technology to arm the immune system against specific infectious diseases. This prophylactic approach has helped fight off chickenpox, measles, influenza, and other pathogens. Vaccines have also profoundly reduced the incidence of polio with only 37 confirmed polio cases in 2016 worldwide[1] and are responsible for the global eradication of smallpox. These advances have radically improved health and quality of life around the globe, but the need for new vaccines continues to grow.

While the conventional view of vaccines is certainly important, there is a lesser known, equally provocative, wave of researching emerging around selective, therapeutic vaccines designed to treat, rather than prevent, non-infectious diseases. In particular, these vaccine-like therapies aim to specifically target tumors – which normally evade the immune system – and to stall autoimmune diseases such as multiple sclerosis (MS) and type I diabetes, diseases in which the immune system erroneously attacks one's own tissues. Important studies in the past decade or so – some of which are highlighted below – make clear that immune cells respond directly to certain synthetic material features. Yet, we are only in the early stages of understanding how materials can be engineered in a rational way to control specific functions of immune cells and tissues;

[†] Adapted from: NM Dold, CM Jewell. "Engineering materials that control the immune system." *CEP Magazine.* **2017**. (in review).

this is the same trial-and-error challenge facing the vaccine and immunotherapy field more broadly. Understanding these fundamental interactions will be important in enabling a new generation of materials that actively program immune response.

Here, we discuss some of the most recent advances in vaccines for infectious diseases and emphasize how new vaccine technologies are being applied for therapeutic applications in cancer and autoimmunity. We introduce approaches that rely on engineered materials and discuss how these biomaterials can modulate immunity. Therapeutic vaccines fit into the broader scheme of immunotherapies that try to correct or enhance the immune system's behavior. For more details of the topics discussed here, the interested readers are referred to recent reviews focused on biomaterials in infectious disease, cancer, and autoimmunity[2–6].

2.2 The basics of a healthy immune response via innate and adaptive pathways

Vaccines for infectious disease arm the immune system against safe formulations of a particular pathogen – protein fragments or killed virus, for example – enabling the body to quickly recognize and destroy this same pathogen during an actual infection. These pathogen-specific responses are faster following vaccination because, vaccines create immunological memory that can last for decades. Achieving such feats requires an elaborate signaling cascade that exploits proportional, integral, and derivative control systems. The immune system must be able to recognize and quickly destroy pathogens

with molecular precision, while avoiding attack or toxicity of self-cells and tissues through a programmed a feature known as tolerance.

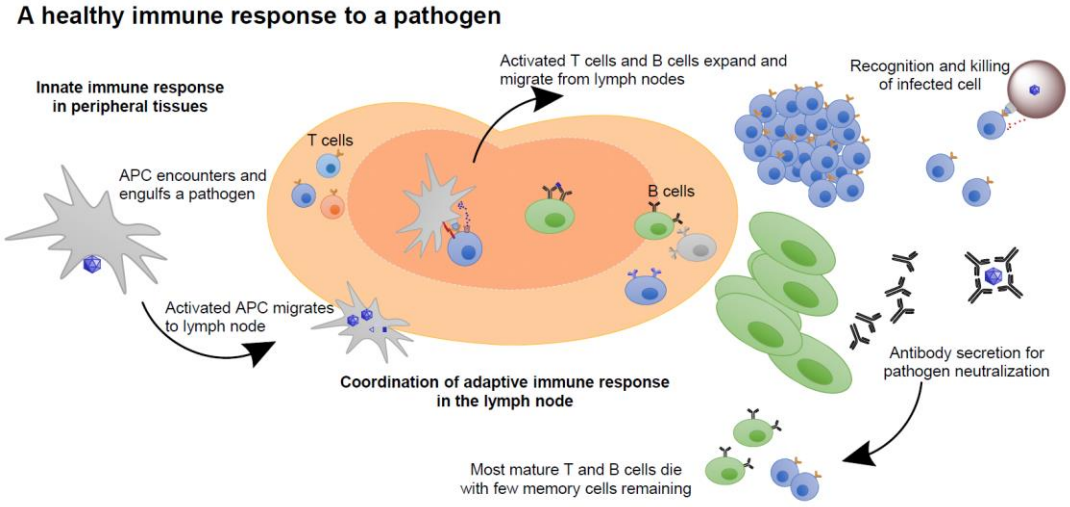

Figure 2.1 Normal immune response to a pathogen
The immune system successfully clears foreign pathogens through cooperation of non-specific innate response that arise faster but lack memory, and highly specific adaptive response that require time to develop initially but create long-lasting immunological memory. Adapted from: NM Dold, CM Jewell. "Engineering materials that control the immune system." CEP Magazine. ***2017****. (in review).*

Foreign invaders can be eliminated because mammalian immune systems have evolved non-specific ("innate") responses that form a first line of defense, along with highly specific ("adaptive") responses that target pathogens and generate memory against pathogens (**Figure 2.1**). Innate immune cells – including macrophages, dendritic cells (DCs), neutrophils, and natural killer cells – can recognize biological patterns that occur in pathogens and are normally absent in human tissues. Some of these include lipopolysaccharides from bacteria and single stranded DNA from viruses. Within minutes and hours of detecting these pathogen-associated patterns, innate immune cells mount responses to directly kill infected cells, phagocytose (i.e., engulf) pathogens, and release signaling molecules called cytokines to signal danger and recruit more immune cells. These processes underpin the inflammation associated with tissues sites

of infection and wounds. Innate immune cells do not possess the capacity for memory, so they share information with cells of the adaptive immune system by digesting and presenting the peptide fragments from digested pathogens. These fragments, called antigens, are presented on specialized proteins called major histocompatibility complexes (MHCI and MHCII) alongside co-stimulatory signals to activate T and B lymphocytes, key players of adaptive immune response. In contrast, presentation of antigen without co-stimulatory signals will not generally trigger response against the antigen. While antigen encounter occurs throughout the body, after encounter, DCs and other antigen presenting cells (APCs) migrate to lymph nodes and spleen to present the antigen to naïve T and B cell residing in these immune tissues. Additionally, free antigen can drain to lymph nodes and spleen for processing by antigen presenting cells and presentation to T and B cells.

Each B cell or T cell has a unique receptor, a B cell receptor (BCR) or T cell receptor (TCR), respectively. BCRs and TCRs are highly specific for a single antigen and determine the specificity of the resulting immune response. Countless BCRs and TCRs exist, but each exists with a very low frequency – roughly 1 of a specific BCR or TCR per 10^5-10^6 lymphocytes – prior to binding the corresponding antigen. When pathogen reach a lymph node, innate immune cells present the processed antigen to a TCR via one of the MHCs, whereas BCRs can detect the pathogen without the aid of antigen presentation. Yet, B cells often require the aid of helper T cells to be fully activated and matured. Helper T cells are activated by DCs and other innate cells presenting antigen on MHC II, while other cytotoxic T cells – those able to directly combat

pathogens – are activated through antigen presentation in MHCI. This complexity highlights a small fraction of the diverse number of levers regulating the immune system.

Once activated, B cells and T cells specific to the antigen being presented divide, expand tremendously to a frequency of up to 1 in 3 lymphocytes depending on cell type. B cells mature and secrete antibodies that can neutralize extracellular pathogens or identify pathogen for destruction by other immune mechanisms. Cytotoxic T cells carry out effector functions by directly seeking and destroying pathogens and infected host cells. Importantly, a fraction of these cells remain in the body after a pathogen is cleared, leaving up to 100-fold more pathogen-specific lymphocytes than the naïve state. These persistent cells provide the immune system with *memory* of the pathogen, allowing lymphocyte populations to expand against previously encountered pathogens much faster during re-exposure. Generation of this protective memory – the goal of most traditional vaccines – is not always efficient or long lasting, which is why multiple immunizations may be required over a short period of time (e.g. hepatitis vaccines), and why adults receive periodic booster shots for certain diseases (e.g. tetanus). More information about immune responses beyond this brief overview can be read in [7–9].

2.3 Dysregulation of immunity in autoimmune diseases and cancer

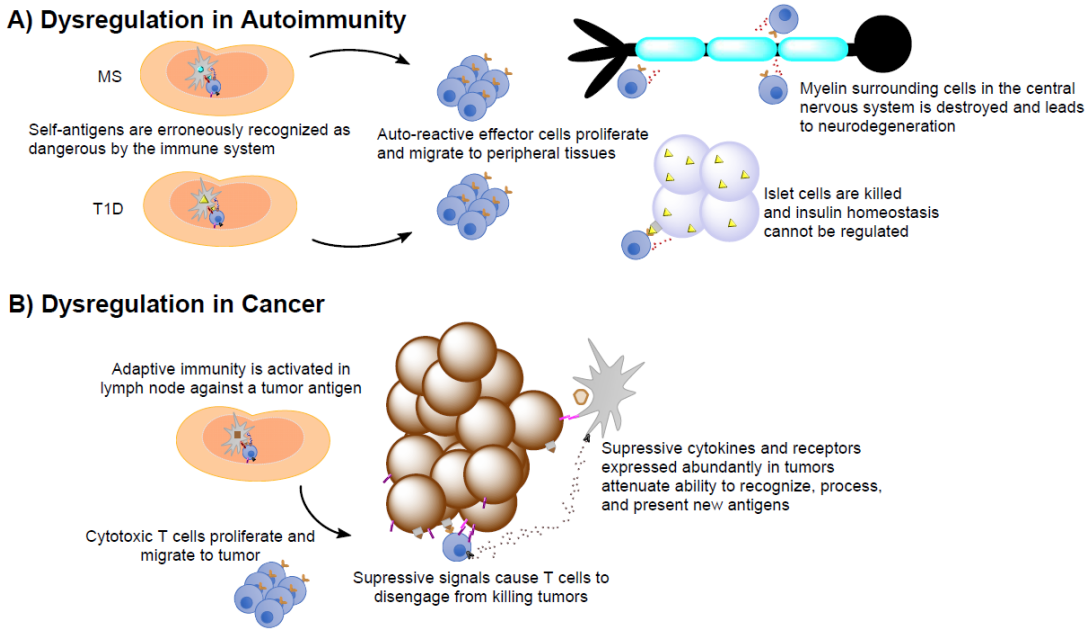

Figure 2.2 Immune dysregulation in autoimmunity and cancer
*Dysregulation of biological signals can cause immune cells to attack one's own tissues in autoimmune diseases (A) or to ignore unhealthy cancerous tissues that needs to be cleared by the immune system (B). Adapted from: NM Dold, CM Jewell. "Engineering materials that control the immune system." CEP Magazine. **2017**. (in review).*

Unfortunately, the normal immune processes just discussed can fail, with cancer and autoimmunity representing two pervasive examples. Autoimmune diseases occur when immune cells inappropriately target one's own cells as if they were foreign or infected. Some of the most common autoimmune diseases are multiple sclerosis (MS), type 1 diabetes, rheumatoid arthritis, and lupus. In MS, for example, the immune system degrades the myelin sheath around neurons, leading to neurodegeneration. In type 1 diabetes, pancreatic islet cells that produce insulin are killed and blood sugar levels become dysregulated. Consequently, therapies that direct the immune system to stop attacking specific "self" molecules could have the potential to stop or reverse autoimmune disease without the broad suppression characteristic of many existing treatments (**Figure 2.2 A**).

In an opposite setting, during cancer, unhealthy cells lose metabolic control and divide in an unrestrained manner. Cancer cells are able to avoid attack by the immune system by presenting and secreting suppressive signals to immune cells. Therefore, even if a T cell is activated against a cancer antigen and infiltrates a tumor, the tumor may signal the T cell to ignore the tumor (tolerance) or the tumor may develop new self-antigens not recognized by infiltrating cells. Moreover, cancer vaccines aimed at generating tumor-specific T cells must be cautious, as there is a risk of lymphocytes recognizing non-cancerous tissues. Effective cancer vaccines must therefore program the immune system to recognize tumor with a high degree of specificity, and to overcome the tumor's immunosuppressive microenvironment (**Figure 2.2 B**).

Regulating the immune system's overzealous mistakes in autoimmunity and its lack of action toward cancer presents a multitude of opposing challenges. Below, we discuss some of the insight gained from biomaterials in the context of prophylactic vaccines for infection disease before discussing new studies building on this knowledge to tackle cancer and autoimmune disease with therapeutic vaccines.

2.4 Biomaterials in conventional vaccines

Vaccines for infectious disease generate memory against a particular pathogen using attenuated pathogens (e.g. modified by chemicals or heat), or specific antigens isolated or derived from the pathogen. Consequently, most vaccines formulate antigens alongside additives – known as *adjuvants* – that exhibit immunostimulatory properties.

Oil-in-water emulsions and aluminum compounds, both biomaterials that adsorb antigens, have been used since the early 20th century.[10] Surprisingly, it's only in the past few decades that adjuvant properties have been interrogated in-depth with respect to materials characterization to reveal particulate size distributions, surface charges, and interactions with innate immune cells[11]. Newer adjuvants on the market include liposomes/virosomes and monophosphoryl lipid A (MPL), a molecule that binds a pathogen recognition receptor from the toll-like receptor (TLR) family[10]. Interestingly, in the case of the recently developed HBV and HPV vaccines, MPL is adsorbed onto aluminum hydroxide, presumably taking advantage of each compound's immunostimulatory mechanisms. Conventional vaccines adjuvants are further reviewed in [10].

Biomaterials offer unique features that could enable a new generation of vaccines and immunotherapies. Interestingly, recent studies reveal that many biomaterials are not immunologically inert, instead exhibiting physiochemical features (e.g., shape, charge, chemical functionality) that interact with immune signaling pathways. For example, polymers such as poly(lactide-*co*-glycolide) (PLGA) and poly(styrene)[12], polyanhydrides[13], and poly(β-amino esters)[14] are all capable of stimulating innate immune responses. Biomaterials also benefit from well-known drug delivery and tissue engineering features unavailable with traditional vaccines such as co-delivery, cargo protection, targeting moieties, and controlled release. All of these features can be harnessed for infectious disease, as well as cancer and autoimmunity. In autoimmunity for example, one new materials approach involves delivering immunosuppressive

molecules along with self-antigens to restore tolerance against these antigens. In cancer, new strategies are harnessing biomaterials for personalized vaccines that maintain anti-tumor immunity within immunosuppressive tumors while avoiding unregulated responses that could damage healthy tissue. Below we highlight four broad delivery approaches – particulate formulations, implanted scaffolds, microneedles, and self-assembled immune cues – that are revealing new lessons that could help transform vaccines and immunotherapies (**Figure 2.3**).

2.5 Particulate formulations enhance bioactivity of vaccine components through controlled release and physical interactions with immune cells

As described above, most conventional vaccines are delivered in a poorly localized or largely soluble dose, while few rational design approaches have been implemented for either conventional or biomaterial-based vaccines and immunotherapies. Yet, the immune system benefits from the physiochemical properties of particles and the other general advantages just mentioned. PLGA is a popular choice for particle delivery, in part because of past precedent as a material for use in humans and the tunable degradation properties achieved by controlling the relative composition of lactide to glycolide polymer subunits. PLGA also offers co-encapsulation and stabilization of hydrophobic and hydrophilic cargos using a simple double-emulsion method. Exploitation of materials to improve the stability and robustness of existing vaccines is one important emerging trend (**Figure 2.3 A**). In one recent example, the inactivated polio virus was combined with excipients – sugars, gelatin, salts – to preserve the integrity of the vaccine during sonication and dehydration.[15] A soluble methacrylate

copolymer (Eudragit® E PO) was added to enable release of two distinct bursts separated by 2-3 weeks. This control demonstrates another emerging principle, controlling delivery kinetics to mimic priming and booster injections with a single treatment (**Figure 2.3 B**). This advance could greatly improve patient compliance, catalyzing a transformative impact in regions with limited access to medical care.

Vaccines may be the next line of defense against virulent bacterial diseases like methicillin resistant *Staphylococcus aureus* (MRSA), which no longer respond to many antibiotic treatments. Wang and colleagues developed a MRSA vaccine by coating PLGA nanoparticles with red blood cell membranes and by doping the membrane with α-hemolysin – one of the toxins expressed by MRSA[16]. Mice treated with the vaccine produced antibody responses against the toxin, and when exposed to MRSA, exhibited reduced bacterial colonization and disease progression owing to neutralization of the toxin by the antibodies. Vaccine-based approaches for bacterial infections are poised to become more important as strains become increasingly resistant to antibiotic regimens.

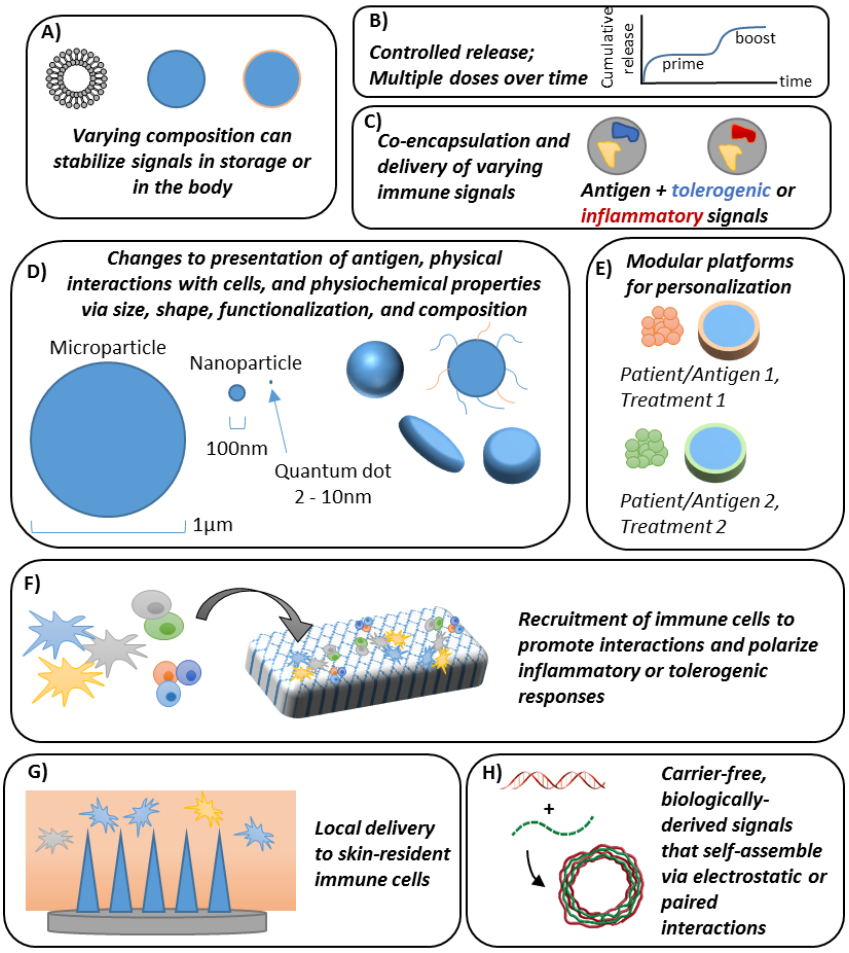

Figure 2.3 Benefits of biomaterial delivery vehicles in vaccines
*Biomaterial particles (A-E), scaffolds (F), microneedles (G), and self-assembled structures (H) have unique advantages that can promote desired immune functions. Adapted from: NM Dold, CM Jewell. "Engineering materials that control the immune system." CEP Magazine. **2017**. (in review).*

In the area of immune tolerance to combat autoimmunity, simple cargo encapsulation and controlled release kinetics are also experiencing a revitalization as important features. One approach involves co-encapsulation of self-peptides, such as the myelin peptides attacked during MS, with regulatory immune signals in nanoparticles (**Figure 2.3 C**). The goal is to reprogram T cells during self-antigen presentation to expand T cells specific for the self-antigen that exert a regulatory function that enables control disease with vaccine-like specificity[17,18]. These approaches require nanoparticle encapsulation and have demonstrated promising therapeutic effects in stopping or

reversing disease in mouse models of MS, allergies, and other inflammatory states. Another platform being developed involves co-encapsulation of peptide and tolerizing drugs into microparticles.[19] These particles are injected directly into lymph nodes of mice and designed to be too large to drain away, creating a local depot that reprograms the microenvironment of these tissues. Of note, a single lymph node treatment permanently reversed disease in a mouse model of MS in a myelin-specific manner.

Also in the context of autoimmunity, several particle strategies seek to change how self-antigens are processed to selectively restore tolerance[20–23]. These approaches involve delivering self-antigen, in various particulate forms, to antigen presenting cells expressing scavenger receptors or other features associated with clearance of apoptotic self-cells, to which tolerance is generally required (**Figure 2.3 D**). Thus, nanoparticles are being used to co-opt natural regulatory pathways, another important theme in the immune engineering field. Several new studies in this general area seek to define the specific design features needed for tolerance. In one approach using a mouse model of MS, uniform quantum dot decorated with defined densities of self-peptides were used to reveal that delivering many quantum dots, each with a low density of peptide, is more effective in promoting tolerance compared with fewer quantum dots each displaying a high density of peptide.[22] The Santamaria lab has developed an approach to directly control how self-antigen is presented to T cells using iron nanoparticles displaying self-peptides in MHCs[24]. Work reported with this system reveals the dose of self-antigen/MHC determines the extent of expansion of antigen-specific T cells, while the density of these complexes determines the polarization of the expanding cells

toward regulatory T cells).[25] These types of fundamental studies will be increasingly important in supporting more rational and efficient design approaches as the complexity of new therapies increases.

In the cancer field, an important emerging trend is the use of biomaterials to create candidates for personalized cancer vaccination (**Figure 2.3 E**). Kuai and colleagues decorated nanodiscs formed from synthetic high-density lipoproteins, a small protein domain, and cholesterol-modified nucleic acid molecules that serve as adjuvants by activating TLR pathways. Multiple peptide tumor antigens could be readily attached to these nanodiscs vaccines.[26] These vaccines were not only effective in expanding T cells against a well characterized model peptide antigen to prevent tumor growth in mice, but importantly, could be assembled using new tumor peptides identified from sequencing mouse tumor cells. When these personalized nanodiscs were delivered with in combination with two gold-standard immunotherapies, the treatment led to complete regression of tumors in nearly all mice compared to less than half in groups receiving soluble versions of the vaccine along with the immunotherapies. Using biomaterials as flexible platforms for quickly customizing cancer vaccines and immunotherapies (e.g., by simply switching peptide antigens or other components) has significant implications for personalized medicine by exploiting the specific antigens or other features of a patient's own tumor.

2.6 Implanted scaffolds recruit immune cells and program pro-inflammatory or tolerogenic responses

Implanted scaffolds enable cell recruitment and can act as a classroom, similar in some ways to lymph nodes or spleen, where innate and adaptive immune cells can interact to promote a desired function or phenotype (**Figure 2.3 F**). These approaches are also drawing on innovations in the tissue engineering field, where recent studies are revealing the role of adaptive immune cells in responding to implants[27] and key immune signaling pathways that help determine how the body will respond to polymers or other foreign bodies[28].

One early example of engineered scaffolds to promote and control immune response involved a macroporous PLGA matrix loaded with tumor lysates, a pro-immune recruitment molecule (GM-CSF), and CpG – synthetic DNA that activates immune function. In mice, DCs were successfully recruited to this site, subsequently migrating to lymph nodes and initiated T cell responses that conferred prolonged survival during tumor models that were typically fatal[29]. More recently, a spontaneously assembling scaffolds with larger pores were prepared using high aspect ratio mesoporous silica rods to recruit innate immune cells – particularly DCs.[30] Recruitment was highest in scaffolds assembled with the greatest aspect ratios, which correlated to larger pore sizes to accommodate recruited cells. Moreover, scaffolds loaded with a model antigen, OVA, and the immune signals described in the previous enabled release of each component over a period of weeks. When applied to mice bearing a tumor cells that express the OVA antigen, 90% of the mice treated with the full vaccine were still alive

when untreated mice had succumbed. This example demonstrates the integration of multiple emerging findings from the immune engineering field – tailored physicochemical material features, sustained release, and adjuvant selection – to provide better control over immune cell recruitment and function. Others are using scaffolds to directly deliver and sustain, rather than recruit, immune cells for anti-tumor immunity – an approach that combines materials with the adoptive cell therapies discussed in this issue[31].

With an opposite goal – restraining immune function – one recent approach sought to treat autoimmunity in a mouse model of type I diabetes using a layered scaffold constructed from a 5mm diameter PLGA disk.[32] This approach involves transplantation of functional pancreatic islet cells – cells destroyed during diabetes – to produce insulin and restore control of blood glucose. However, immune tolerance is required to prevent these new islet cells from meeting the same fate as the original islets in the host mouse: destruction by malfunctioning self-reactive immune cells. Thus, the outer disc layers were porous to support islet cell seeding, while an inner solid PLGA layer contained transforming growth factor-beta 1 (TGF-β1). TGF-β1 is known to reduce antigen presentation by innate cells and to promote differentiation of T cells into tolerogenic regulatory T cells. Scaffolds loaded with TGF-β1 and islets extended islet cell function and lowered inflammatory cytokine secretion compared to mice receiving scaffolds lacking TGF-β1. By exhibiting control over local inflammation at the site of transplantation, this approach motivates additional vaccine strategies that deliver other signals locally to control the immune environment in and around transplant sites.

2.7 Microneedles deliver vaccines with local precision, cargo stability, and increased compliance

Microneedle arrays are alternatives to hypodermic needles that deliver cargo loaded in or on the surface of dozens of micro-scale features, each several hundred microns in height (**Figure 2.3 G**). At this size scale, application is nearly painless because the microneedles reach few pain receptors. Their small size also confers other unique properties: microneedles can efficiently deliver cargo intradermally to skin-resident immune cells. A recent first-in-humans phase I clinical trial demonstrated 650μm dissolvable microneedle arrays could be used to effectively deliver the inactivated influenza vaccine.[33] Interestingly, the arrays could be stored in unrefrigerated conditions, self-administered by patients, and discarded following use more safely than traditional sharps.

Another important area microneedles are being developed for is DNA vaccination, which relies on expression of antigens encoded in DNA such that cells internalize and express an engineered DNA vector to display or secrete the antigen of interest. Demuth and colleagues demonstrated the utility of coated polymer microneedle arrays to release DNA alongside adjuvants and excipients that promote transfection.[34] Arrays molded from poly(L-lactide) (PLLA) were layered with four distinct polyelectrolytes: (1) a polymer responsive to both light and pH to promote release from the needle surface, (2) an immunostimulatory adjuvant that mimics viral RNA, (3) poly(β-amino esters) known to promote transfection, and (4) plasmid DNA encoding antigen from HIV or

fluorescent reporters. The anionic nucleic acids and cationic polymers formed polyelectrolyte multilayers on the array's surface, and sustained release of antigen and adjuvant following application of the array to mice and non-human primate skin. In mice, immune responses against the antigen were comparable to those induced by DNA vaccines delivered using electroporation. In primates, the fluorescent reporter demonstrated gene expression orders of magnitude higher than intradermal injection.

More recently, microneedles are being developed for cancer vaccination and combination immunotherapies. For example, Wang and colleagues fabricated hyaluronic acid based microneedles containing dextran nanoparticles that encapsulated the glucose oxidase enzyme to achieve pH responsive release of an important antibody targeting the immunosuppressive PD-1 pathway that tumors use to block anti-tumor response[35]. Thus, delivery of anti-PD-1 prevents tumors from inactivating T cells through PD-1's pathway by blocking this receptor. In another approach, robotic automation was used to coat PLL microneedles arrays with up to 128 nano-scale layers juxtaposing tumor antigens and nucleic acid TLR agonists as adjuvants.[36] In mice, this co-delivery promoted expansion of T cells specifically reactive to the tumor antigen. This first example of microneedle delivery of tumor antigens highlights the ability to combine features from different ends of the design space, automated manufacturing and co-delivery, for example, to control immune responses more precisely. Together, the advances presented in this section show microneedles are already finding clinical utility in infectious disease, while holding exciting potential cancer and autoimmunity.

2.8 Self-assembly of bio-derived immune signals simplifies design

Synthetic biomaterials and existing vaccine excipients may affect the immune system in ways that are difficult to characterize – the intrinsic immune effects already discussed are one important example. Avoiding unanticipated inflammation is especially important in autoimmunity – where inflammation might make disease worse – and in avoiding off-target effects from immunotherapies. Materials made entirely of well-defined immune signals, but that mimic attractive features of biomaterials – such as co-delivery and tunable loading – provide an opportunity for more modular design strategies that also eliminate confounding intrinsic immune effects of polymers or other materials. Self-assembly is well suited for this goal, owing to spontaneous, molecularly defined processes.

An approach developed in our group involves electrostatic self-assembly of immunological polyelectrolytes (i.e. peptide antigen and immune modulating nucleic acids) on a calcium carbonate particle template (**Figure 2.3 H**).[37] The template is subsequently removed with EDTA to create "carrier free" immune polyelectrolyte multilayer (iPEM) capsules. iPEMs enable co-delivery, tunable sizes, and control over the absolute and relative loadings of the antigens and nucleic acids. In mice, capsules built from model tumor antigens and a nucleic acid TLR agonist confer anti-tumor immunity. By exploiting the modularity of this platform, this system has also been extended to autoimmunity.[38] iPEMs built from myelin peptide and a regulatory nucleic acid eliminates disease in a mouse model of MS. These iPEM capsules also

reduced inflammatory cytokines in samples from human MS patients, while iPEMs formed myelin and scrambled nucleic acid did not.

Self-assembled immunological cues can also borrow directly from pathogens. Virus-like particles (VLPs) are constructed from protein subunits of viruses, but they do not include components that can make viruses infectious. These VLPS rely on the intrinsic immunogenicity of viral proteins and can be harnessed in the context of cancer vaccination to combat cancer by co-delivering cancer antigens in the VLP. VLP vaccines are sometimes ineffective if the patient has previously been exposed to the virus proteins because immunity is not directed against the cancer antigen. Consequently, several are investigating use of viral proteins that humans do not commonly encounter such as those derived from bacteriophages[39] and plant viruses[40]. In one example, a carbohydrate tumor antigen that is normally a difficult target for the immune system was attached to the surface of a bacteriophage subunit, and it induced substantial antibody production against the antigen in mice[39]. An approach using a plant virus particle induced similar antibody responses against a lymphoma protein antigen while substantially enhancing survival of mice[40].

Other researchers are working to design vaccines with self-assembling peptides overexpressed in tumors. A recent example from Sun and colleagues using MUC1 glycopeptides with two adjuvants – CpG ODN and Pam_3CSK_4 (a TLR1/2 stimulant) – involved electrostatic assembly of a library of particles using different combinations of and slight variations to the structure of each component.[41] They reported significant

increases to inflammatory cytokine secretion and antibody secretion. Finally, Hudalla and colleagues engineered protein moieties that can self-assemble into nanofibers, while exposing multiple different proteins along the length of the fibers[42]. This approach was successful in inducing significantly higher antibody responses against the engineered protein fibers in comparison to soluble forms. Although each of these strategies for self-assembly of immune signals are still in the pre-clinical phase, they represent an exciting frontier for exerting exquisite control over immune function without the worry of unanticipated effects from excipients.

2.9 Outlook

The complexity of the immune system and the diversity of biomaterials available for vaccine development are enormous. This complexity underscores the need for fundamental studies that reveal the role of specific design parameters. Interdisciplinary partnerships are also needed to combine immunology expertise with engineering expertise in materials design and characterization. Additionally, the expertise of process and quality engineers will be vital because many of the strategies employed in pre-clinical studies will require significant resources to scale up in a manner that meets applicable regulatory standards for human use.

Perhaps the greatest challenge for those working on biomaterial vaccines is the balance between understanding immunological mechanisms and eliciting a prophylactic or therapeutic benefit. Do we need to characterize new and existing adjuvants more fully before we champion their use? Or, should striking results that shrink tumors or reverse

autoimmune symptoms be a focus, even at exorbitant cost or inefficient processes? Of course, the answers to these questions is likely a balance: more rigorous analysis in basic studies, in translation, and in manufacturing would be useful in assessing the risks and rewards of these questions. Regardless, materials-based vaccination and immunotherapies are enabling new ground to be broken on pathogenic and non-infectious disease, and we will continue to learn more about exciting potential and most prominent challenges in the coming years. In **Chapter 3**, we discuss the ability of a polymer to stimulate immune responses and its utility as a nanoparticle therapeutic delivery vehicle for nucleic acids.

Chapter 3 : Poly(ß-amino esters) activate mouse macrophages in soluble and nanoparticulate form

3.1 Introduction

Biodegradable polymer delivery vehicles for gene therapies that provide protection against premature nucleic acid degradation, controlled release, and passive targeting have been intensely studied to enhance efficacy and durability of nucleic acid vaccines and therapies. These approaches are generally designed to enhance the expression of proteins that the immune system should target or to act as stimulatory signals by mimicking the nucleic acid structures of viruses or bacteria, which bind immunostimulatory receptors such as toll-like receptors (TLRs)[43,44]. Poly(β-amino esters) (PBAEs) are biodegradable polymers that can complex with nucleic acid cargos through electrostatic condensation owing to the cationic nature of the polymer's amine groups and anionic phosphate backbone of nucleic acids. Together, they can self-assemble into structures such as layered films on microneedles[34] and nanoparticle complexes. PBAEs are known to promote cellular uptake and endosomal escape into the cytosol via the proton sponge effect[45], which could promote interactions with TLRs that are localized to endosomes or to other similar receptors (e.g. RIG-I, MDA5[46]) localized in the cytosol. PBAEs also can be synthesized with varying features (e.g. molecular weight, end groups, etc.) that may affect intracellular delivery – i.e. transfection efficiency – and interactions with individual cell types [14,45,47–51].

Because nucleic acid cargos can have off-target effects including immune stimulation[52,53] and because PBAEs can exhibit intrinsic immunogenicity, it is vital to understand the ability of these materials to either mitigate or enhance pro-inflammatory signaling. In the context of immunotherapies and vaccines for cancer or infectious disease, activation of the immune system is a desired effect when it remains under control; however, immunostimulatory effects can be undesirable when they thwart attempts to suppress pro-inflammatory signaling to prevent transplant rejection or autoimmune diseases.

Antigen presenting cells (APCs) such as dendritic cells (DCs) and macrophages are innate immune cells that surveil the body for pathogens and damaged tissues. These cells are important players in the response to biomaterial vaccine carriers. When these cells encounter immunostimulatory signals – biological patterns that appear in pathogens, but not in humans – APCs coordinate the immune response by phagocytosing and presenting antigen molecules to lymphocytes in lymph nodes, which initiate the adaptive immune response[54]. Consequently, polymeric delivery vehicles that activate specific functions in APCs are valuable tools in targeted stimulation of the immune system for vaccines and immunotherapies that require pro-inflammatory responses.

Particles are attractive vehicles for vaccine delivery because they can be formulated into different sizes and shapes that generally encourage interactions with APCs through phagocytosis[55,56], and they can promote gene transfection[57]. Moreover, polymeric

particles can directly enhance activation of immune pathways via intrinsic immune effects through a range of inflammatory pathways including: the NALP3 inflammasome[12], toll-like receptors (TLRs) and MyD88 signaling[58], IRF-dependent signaling[59], and complement[60,61].

Our lab has previously used primary DCs to show that PBAEs exhibit some intrinsic immune function when in particulate form following complexation with a polyanion, poly(sodium 4-styrenesulfonate); PBAE degradation[14] and molecular weight[51] played roles in the nature of the immune response to these particles. Because PBAEs were designed and characterized as nucleic acid delivery vehicles[45,47], we extend our studies here to nucleic acid delivery using a different *in vitro* model of immune activation: the RAW264.7 mouse macrophage cell line. RAW264.7 cells are a popular *in vitro* model for innate immune responses to biomaterials because they are a well-established cell line that exhibits behaviors similar to primary APCs[62]; they are also recommended for use in international standards for implanted biomaterials testing[63]. Moreover, macrophages represent an alternative therapeutic target for particles that stimulate immune responses against diseases like cancer because they reside in all tissues and have unique capabilities in phagocytosing and clearing particles and/or cellular debris[64,65].

Another area of particular interest in nucleic acid delivery for immunotherapy is RNAi, which can be carried using small interfering RNAs (siRNA)[66,67]. These short, double stranded RNAs cause degradation of target mRNAs through the RISC complex, and

they generally lead to lower expression of the associated protein. Therefore, RNAi could be used to attenuate activity of immune checkpoint molecules (e.g. CTLA-4, PD-1, TIM-3), which are overexpressed in tumor microenvironments and suppress immune cell activity against tumors[68]. Silencing these checkpoint molecules could restore function to immune cells and promote tumor killing.

To avoid sequence-specific RNAi effects when examining intrinsic effects of PBAE and siRNA delivered by these polymers, we selected a commercially available dicer-substrate siRNA (DsiRNA a form of siRNA with enhanced silencing activity[69]) duplex (NC1, from Integrated DNA Technologies) that does not target any part of the mouse or human transcriptome. Here, we investigate the intrinsic ability of PBAE to enhance pro-inflammatory pathways in both soluble and particle form. For particle studies, we show that PBAEs and DsiRNA can be assembled into nanoparticle complexes with tunable size and charge. We also show that PBAEs activate RAW264.7 cells in both particulate and soluble form. Further, we provide data suggesting this activation arises independently of two important inflammatory immune pathways, those of NF-κB and IRF.

Finally, we show that the RAW264.7 cell line can be used as a model for RNAi silencing of immune checkpoint molecules because they express the TIM-3 immune checkpoint. Stimulating tumor associated macrophages while silencing checkpoint expression would reduce the immunosuppressive effects of checkpoint molecules that are overexpressed in cancers and restore functions to macrophages, which could further

stimulate tumor killing by T cells via cytokine expression and pro-inflammatory antigen presentation[64,70]. Using a commercial transfection reagent, we show that DsiRNA can be used to effectively attenuate TIM-3 expression and modulate immune function. Together, these studies motivate future work involving PBAEs as an immune adjuvant and the RAW264.7 cell line as model for immune checkpoint studies in cancer models.

3.2 Materials and Methods

3.2.1 Materials

PBAE was synthesized in a Michael-type addition reaction using standard methods previously described[14]. DsiRNAs were purchased (Integrated DNA Technologies) and resuspended at 20μM in nuclease free water. Dulbecco's modified eagle medium (DMEM) and fetal bovine serum (FBS) were purchased from Gibco and Corning, respectively. Antibiotics – Normocin and Zeocin – and low molecular weight polyinosinic-polycytidylic acid (LMW polyIC) were purchased from Invivogen. Lipofectamine RNAiMAX was purchased from ThermoFisher Scientific. Sodium acetate buffer was purchased from Sigma-Aldrich. Antibodies for maturation markers (CD40, CD80, and CD86) and for Fc receptor blocking were purchased from BD Biosciences. A mouse IL-6 ELISA set was purchased from BD Biosciences. Antibodies for TIM-3 were purchased from BioLegend.

3.2.2 Cell culture

RAW264.7 cells and RAW-Dual (IRF-Lucia/KIN-[MIP-2]SEAP) cells were purchased from ATCC and Invivogen, respectively. Both cell types were maintained in DMEM containing 4.5g/l glucose and 4mM l-glutamine, and the media for both cell types was supplemented with 10% FBS. For RAW-Dual cells only, antibiotics were added per the supplier's recommendation with Normocin at 100µg/ml for all passages and Zeocin every other passage at 200µg/ml to maintain selective pressure. Cells were grown in tissue culture-treated polystyrene flasks, while experimental treatments in 96-well plates were performed using non-treated polystyrene. RAW-Dual assays were performed without either antibiotic following a passage containing both Normocin and Zeocin.

3.2.3 Nanoparticle complex formulation

Nanoparticles were produced by complexation of PBAE and DsiRNA in 25mM sodium acetate buffer (NaAc, pH 5). All buffer solutions for complex formation were filtered (0.2µm). Complexes were formed at varying w/w ratios while v/v at a constant 1:1 with each component – polymer and DsiRNA duplex – added in 25µL volumes for 50µL total volume per batch. DsiRNA duplexes were diluted to 40µg/mL for 1µg in 25µL NaAc, and PBAE solutions were serially diluted to vary the w/w ratio of a complex components following 0.2µm filtration of PBAE in solution at either 2mg/mL or 1mg/mL. Complexes were mixed vigorously by pipetting and used immediately for either physiochemical characterization or cell treatments.

3.2.4 Nanoparticle size and zeta potential measurements

Dynamic light scattering (DLS, size) and electrophoretic light scattering (ELS, zeta potential) were performed using a Malvern Zetasizer Nano ZS90. Measurements were performed in disposable 50µL cuvettes and capillary cells for DLS and ELS, respectively. ELS measurements were conducted using the diffusion barrier technique[71]; briefly, immediately following DLS, sample was transferred from the disposable cuvette and concentrated at the bottom of a capillary cell previously filled with NaAc using a flexible gel-loading pipette tip.

3.2.5 Quantification of macrophage cell line activation by flow cytometry

RAW264.7 cells were passaged (no greater than P10) by cell scraping and seeded at 50,000-55,000 cells per well for all experiments in 96-well plates on top of prepared treatments (e.g. complexes, soluble polymer or RNA, TLRa). At 24 and 48 hours, cells were collected and, after blocking the Fc receptors, were stained with fluorescent antibodies for surface activation markers (i.e. CD40, CD80, and CD86) and with a viability dye (DAPI). Flow cytometry (BD FACSCanto II) was used to determine relative levels of activation through analysis using FlowJo (v.10.2, TreeStar, Ashland, OR). Cell supernatants were saved for analysis by ELISA.

3.2.6 Immune pathway characterization in RAW-Dual reporter cell line

RAW-Dual cells were prepared and treated in the same manner as RAW264.7 cells described above. Following 24 or 48 hour incubation, supernatants were collected and aliquots were tested for the secreted Lucia luciferase and secreted embryonic alkaline

phosphatase (SEAP) reporters (IRF and NF-κB, respectively) using Invivogen's QUANTI-Luc and QUANTI-Blue detection reagents with values were recorded for luminescence and absorbance per manufacturer's protocol.

3.2.7 TIM-3 knockdown screening in macrophage cell line

RAW264.7 cells were reverse transfected with TIM-3 targeted and NC1 DsiRNA duplexes prepared using Lipofectamine RNAiMAX per manufacturer's instructions. Transfection was carried out in 96-well plates with 20,000 cells per well plated on untreated surfaces over the treatments for a final concentration 10nM DsiRNA. After blocking the Fc receptors, surface expression of TIM-3, CD40, and CD80 among live ($DAPI^-$) cells was quantified by flow cytometry using fluorescent antibodies.

3.2.8 IL-6 ELISA

Cell supernatants were collected during flow cytometry experiments. ELISA against IL-6 was performed according to manufacturer's instructions (BD Biosciences) with 5x dilutions, except for LPS-treated samples, which were diluted 10x. Standard curves were generated for using a five-parameter logistic model in GraphPad Prism 7.

3.2.9 Statistical analysis

Multiple pairwise comparisons were performed using the Tukey method in Minitab 17 with a p-value less than 0.05 indicating significance. All error bars are reported as standard error of the mean (S.E.M.) unless stated otherwise.

3.3 Results

3.3.1 PBAE/RNA ratios tune size and charge of complexes

PBAE (**Figure 3.1 A**) and DsiRNA were assembled into particles at varying w/w ratios ranging from 50:1 to 0.5:1 and immediately characterized for size and zeta potential. Nanoparticle complexes formed with diameters between 125nm and 400nm (**Figure 3.1 B**) and zeta potential from -10mV to +22mV (**Figure 3.1 C**) with the most highly charged particles forming smaller particles at the extreme ends of the range of w/w ratios.

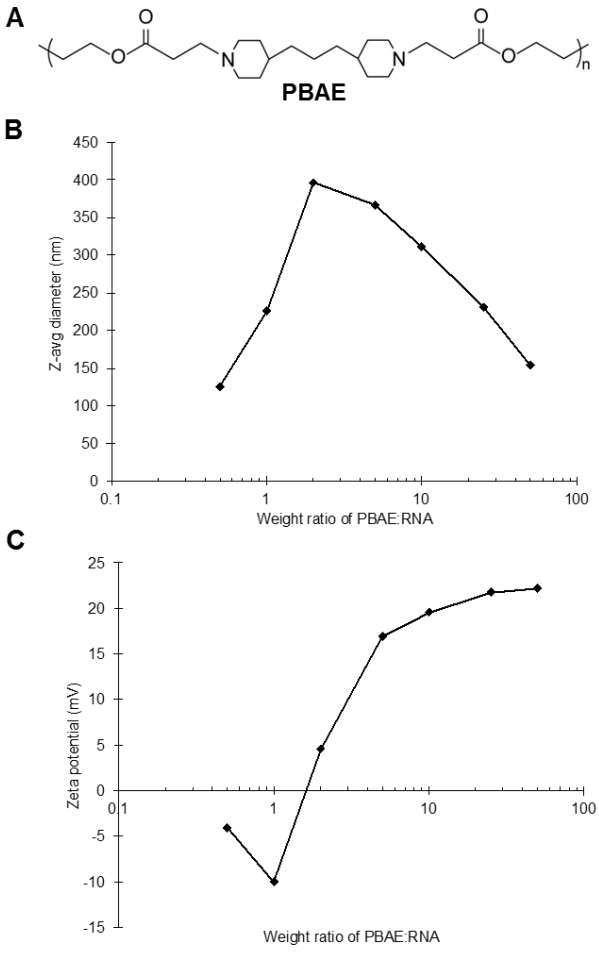

Figure 3.1 PBAE-DsiRNA complex characterization.
*Complexes formed with PBAE (**A**) and DsiRNA in NaAc were characterized for size (**B**) and zeta potential (**C**) at varying weight ratios of PBAE:RNA.*

3.3.2 PBAEs induce RAW264.7 activation in free and complexed form

In our lab's previous studies, free PBAE was unable to activate primary DCs, whereas PBAE particles were able to cause activation[14,51]. In the present studies, we find that PBAE was able to activate RAW264.7 macrophages in both free and complexed form with NC1 DsiRNA as measured by flow cytometry (**Figure 3.2 and Figure 3.3**). RAW264.7 cells in non-adherent 96-well plates were treated with soluble PBAE ranging from 0.5μg/mL to 4μg/mL and complexes from 1μg/mL to 3μg/mL. Complex treatments were matched to equivalent soluble PBAE dose using PBAE:RNA ratios from 0.5:1 to 25:1 (**Table 3.1**). At 24 and 48 hours following treatment, the cells receiving PBAE treatments were compared to cells receiving control treatments of buffer and various TLRas. Soluble PBAE and PBAE-RNA complexes increased expression of all measured markers in a statistically significant, dose-dependent fashion.

We observed only a modest increase in CD40 expression (**Figure 3.3 A,B**) from PBAE, while there were more striking dose-dependent increases in CD80 and CD86 at both 24 and 48 hours (**Figure 3.3 C-F**). Complexed PBAE treatments were no more potent than the soluble form, but they appeared in some cases to contribute to statistically significant decreases in viability similar to that of LPS in statistical significance, but not magnitude (**Figure 3.2 A,B**), which is expected to cause some macrophage cell senescence or death[62,72]. No decreases in viability were apparent with the soluble PBAE treatments.

Table 3.1 Dose matching of soluble and complexed treatments
Soluble (S) and complexed (C) treatments were plated in groups to match soluble PBAE doses with complexes of varying w/w ratios of PBAE:RNA. Dose matching PBAE leads to varying amounts of DsiRNA based on PBAE:RNA ratio.

PBAE µg/mL	**4**	**3**					**2**			**1**				**0.5**
Type	S	S	25:1 C	5:1 C	2:1 C	1:1 C	S	25:1 C	1:1 C	S	25:1 C	5:1 C	0.5:1	S
DsiRNA µg/mL	0	0	0.12	0.6	1.5	3	0	0.08	0.4	0	0.04	0.2	2	0

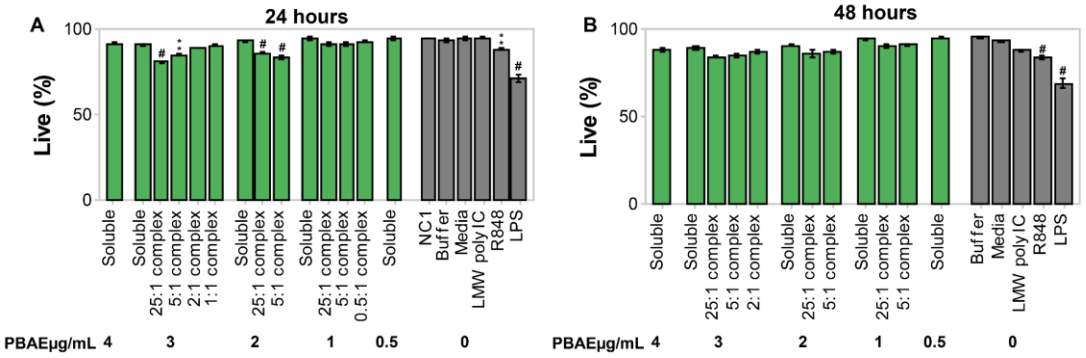

Figure 3.2 Viability of RAW264.7 cells treated with PBAE
RAW264.7 cells treated with soluble and complexed PBAE at specified w/w ratios were assessed for viability (DAPI$^-$) at 24 and 48 hours using flow cytometry. Statistical symbols (p <0.05, **p<0.01, *** or # p<0.001) directly above individual bars indicate significance against equivalent soluble controls for complexes and TLRa. Error bars: S.E.M.*

Additionally, RAW264.7 cells did not mature in response to the TLR3 agonist (TLR3a) polyIC, but they were activated by TLR4a (LPS) and TLR7/8a (R848) (**Figure 3.3 A-F**). LPS, R848, and the highest doses of PBAE also caused drastic changes in cell culture morphology (**Figure 3.4**) – spreading, culture density, and intracellular bodies depending on treatment – whereas polyIC and buffer controls did not appear to be different. Treatments with DsiRNA alone, which can act as a TLRa since it is not chemically modified[53], also did not induce maturation.

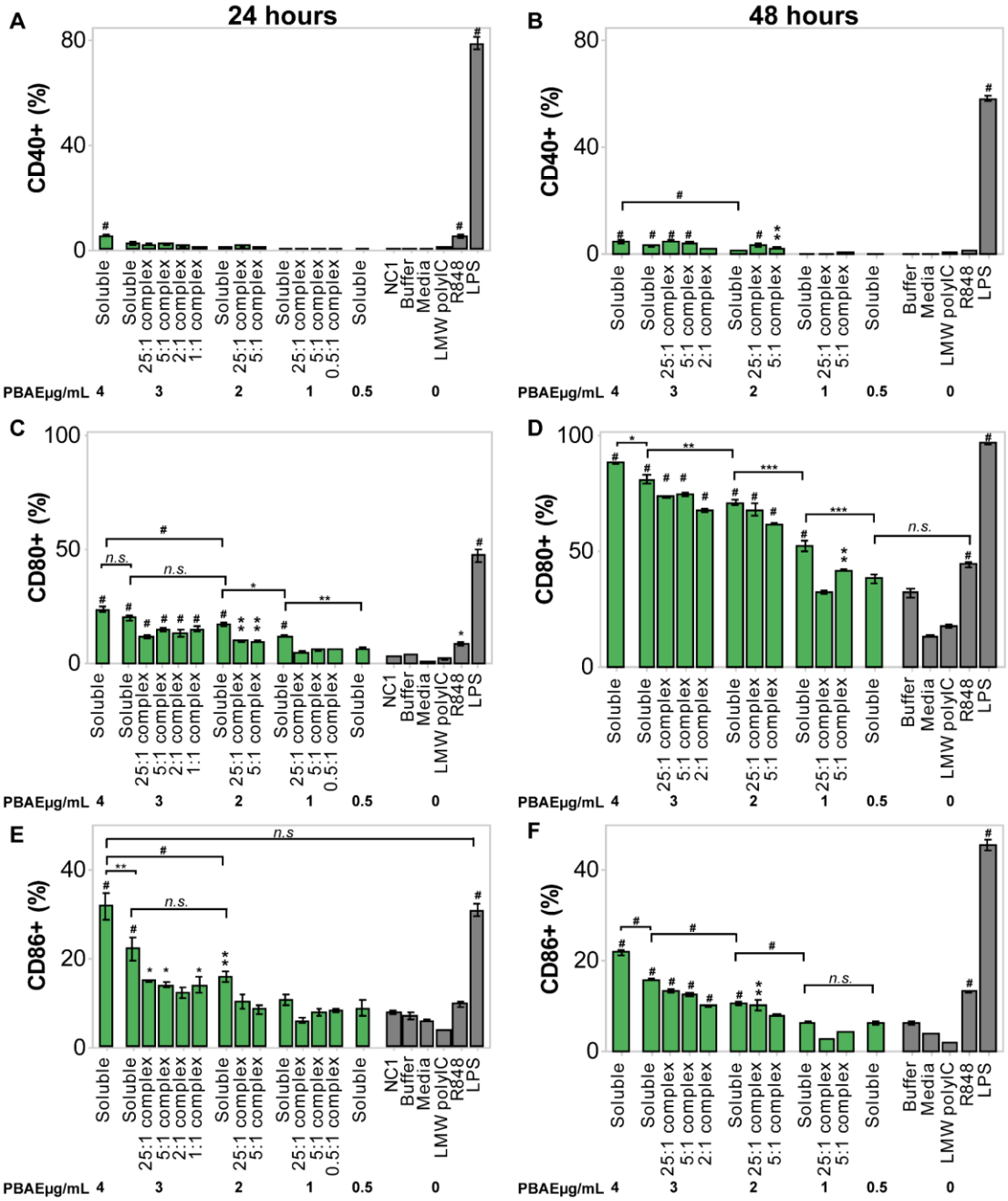

Figure 3.3 RAW264.7 activation at 24 and 48 hours.
RAW264.7 cells treated with soluble PBAE and PBAE complexed with NC1 at PBAE concentrations 0.5μg/mL-4μg/mL (green) and compared to soluble controls without PBAE (gray). Cells were stained with fluorescent antibodies to evaluate surface expression of maturation markers (CD40 (A,B), CD80 (C,D), and CD86 (E,F)) by flow cytometry at 24 and 48 hours among live ($DAPI^-$) cells. Statistical symbols (p <0.05, **p<0.01, *** or # p<0.001) directly above individual bars indicate significantly higher mean than buffer. For clarity, brackets indicate key statistical relationships (using "n.s." for not significant) among soluble treatments only. Error bars: S.E.M.*

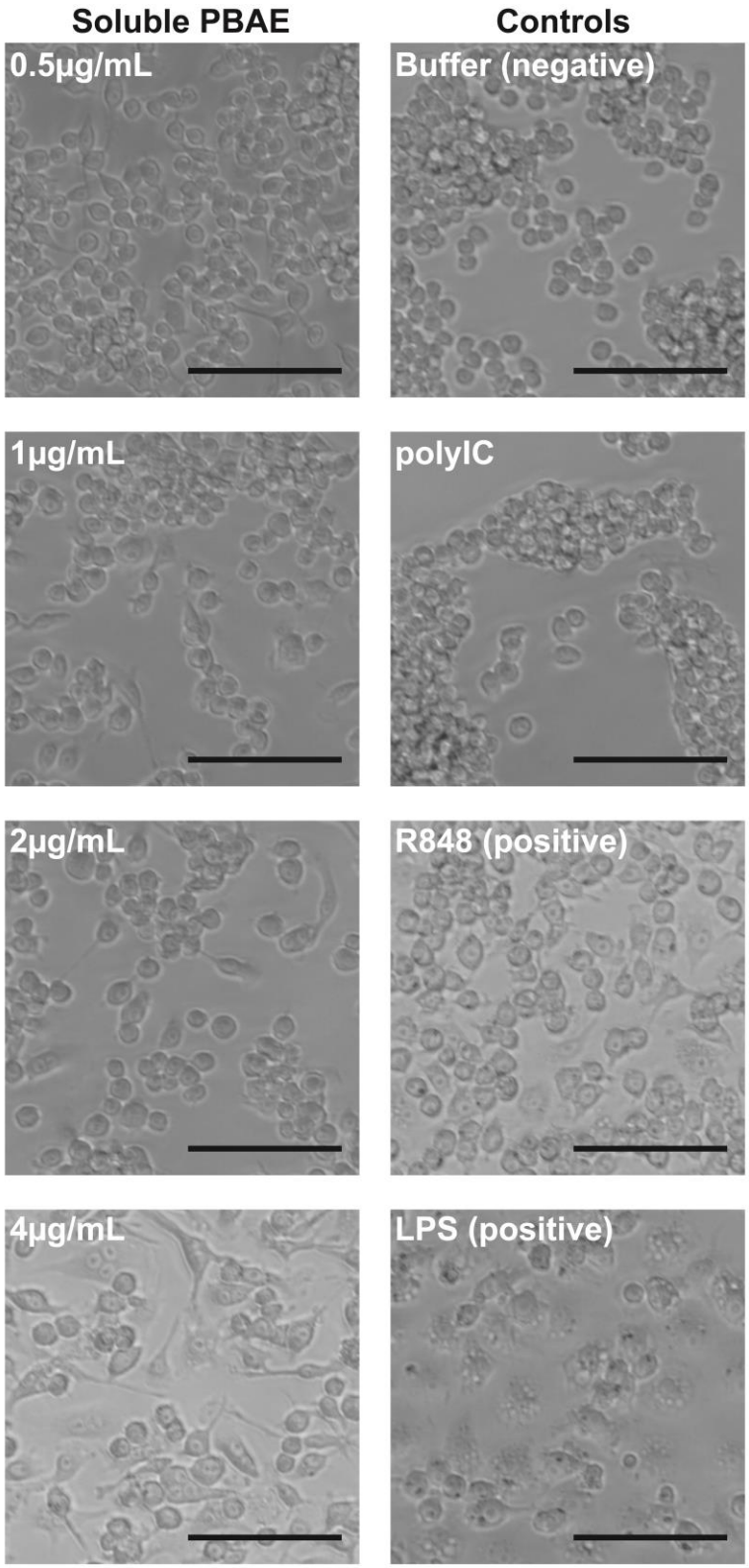

Figure 3.4 RAW264.7 morphology after overnight treatment.
Representative micrographs of RAW264.7 cells (phase contrast, 10X, scale bar: 100µm) following overnight treatment with soluble PBAE from 0.5µg/mL to 4µg/mL and controls (LPS 100ng/mL, R848 1µg/mL, polyIC 10µg/mL, and sodium acetate buffer).

3.3.3 PBAEs do not induce IL-6 secretion

From the samples tested in assays above, cell supernatants were taken for examination by ELISA for IL-6 secretion because IL-6 is implicated in a wide range of pro- and anti-inflammatory pathways in cancer, infection, autoimmunity and injury[73]. Despite induction of IL-6 secretion by both LPS and R848 above baseline levels, PBAE, polyIC, and other controls showed no sign of IL-6 production at either 24 or 48 hours (**Figure 3.5 A,B**). This result suggests that activation of RAW264.7 cells by PBAE is mediated by different pathways than those activated by TLRa such as LPS or R848.

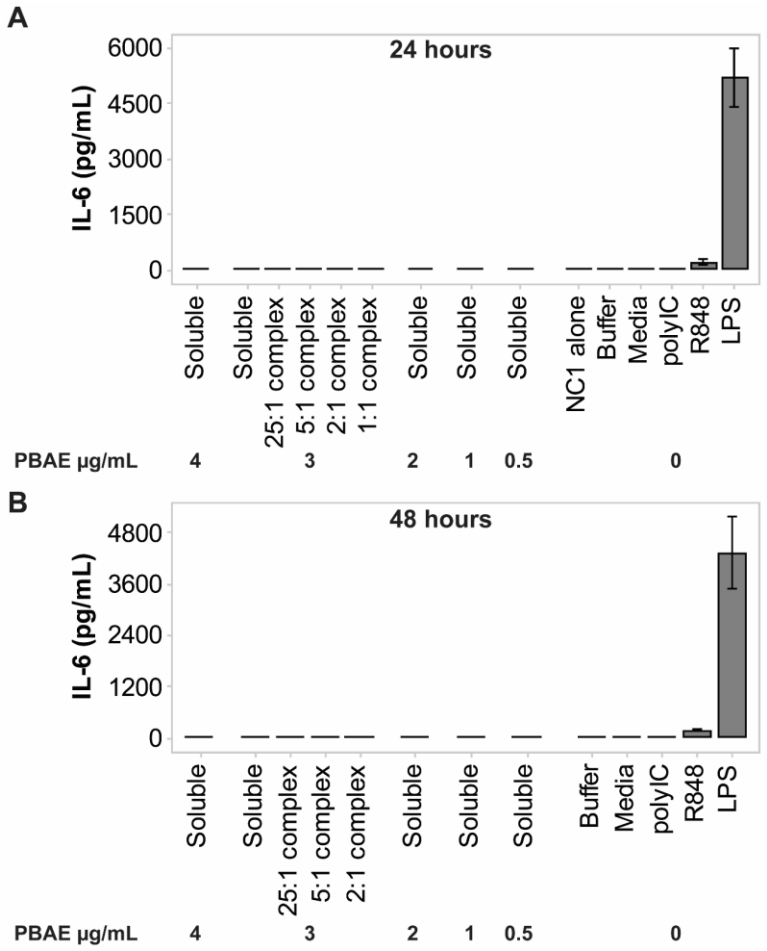

Figure 3.5 IL-6 secretion in RAW264.7 cells at 24 and 48 hours
Secretion of IL-6 was measured by ELISA. Results from soluble treatments of PBAE ranging from 0.5-4µg/mL, complexed treatments at 3µg/mL and controls including TLRa are shown. Error bars: 95% confidence intervals.

3.3.4 PBAEs do not stimulate reporter cells through NF-κB or IRF

Because PBAE appears to activate RAW264.7 cells via a different mechanism than LPS and R848, we decided to quantify transcription factor activity as a more general indicator of RAW264.7 cells' PBAE-induced pro-inflammatory activity mechanism. We hypothesized that PBAE would act through one of the NF-κB and/or IRF families of transcription factors, which respond to a broad array of immune signals[74,75]. To test this idea we used RAW-Dual reporter cells, a cell line chosen for further study of intrinsic immunogenicity because they are derived from RAW264.7 cells. The RAW-Dual cells secrete reporter proteins (secreted embryonic alkaline phosphatase (SEAP) and Lucia luciferase) in response to NF-κB and IRF activity via two independent inducible promoters. Cells were treated with soluble PBAE or LPS as a positive control in the same manner as RAW264.7 cells, and supernatants were collected to assess reporter activity. PBAE treatments that successfully matured RAW264.7 cells did not induce activity through NF-κB nor IRF despite apparent dose-dependent responses of both reporters to LPS (**Figure 3.6**). This result provided further evidence that inflammatory phenotype of PBAE-treated RAW264.7 cells is distinct from those receiving the TLRa used in these experiments.

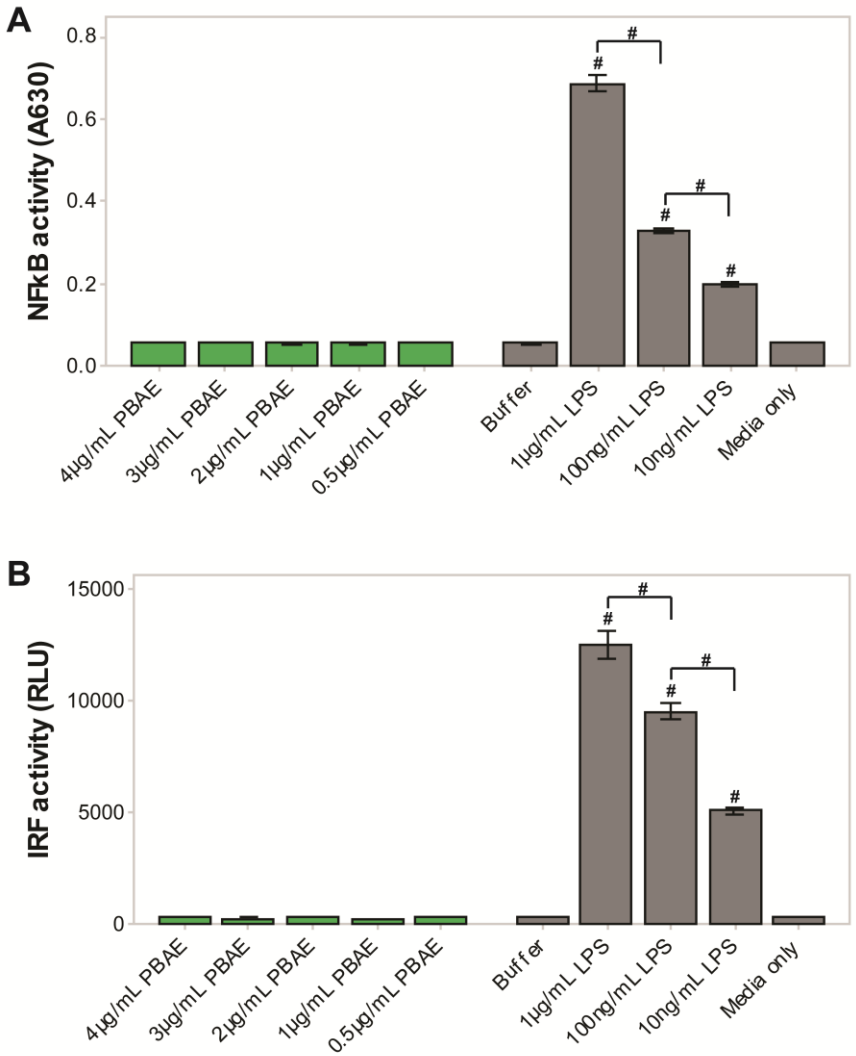

Figure 3.6 Activity in RAW-Dual reporter cells.
Cell supernatants from RAW-Dual cells were screened for NF-κB secreted embryonic alkaline phosphatase (A) and IRF secreted Lucia luciferase reporters (B) in absorbance and luminescence assays following 24 hour incubation with PBAE and controls. Statistical symbols (p <0.05, **p<0.01, *** or # p<0.001) directly above individual bars indicate significantly higher mean than buffer. For clarity, brackets indicate key statistical relationships among treatments as labeled. Error bars: S.E.M.*

3.3.5 TIM-3 silencing alters activation marker expression

To motivate future studies using PBAE in delivering functional DsiRNA moieties, we chose an immunological target, TIM-3. Since TIM-3 is an immune checkpoint implicated in the suppression of tumor-infiltrating immune cells[76–78], and it is often co-expressed with other checkpoint and regulatory molecules such as PD-1 and

FoxP3[79–81], we hypothesized that reducing TIM-3 expression might lead to a more pro-inflammatory phenotype. *In vivo*, this phenotype might restore tumor killing function to cells that are normally suppressed in tumor microenvironments. RAW264.7 cells were set up as an initial model for knockdown of the TIM-3 checkpoint protein, which is expressed on the surface of RAW264.7 cells. Here, we used a commercial transfection reagent (Lipofectamine RNAiMAX) as a preliminary benchmark for future studies with complexes of PBAE and DsiRNA.

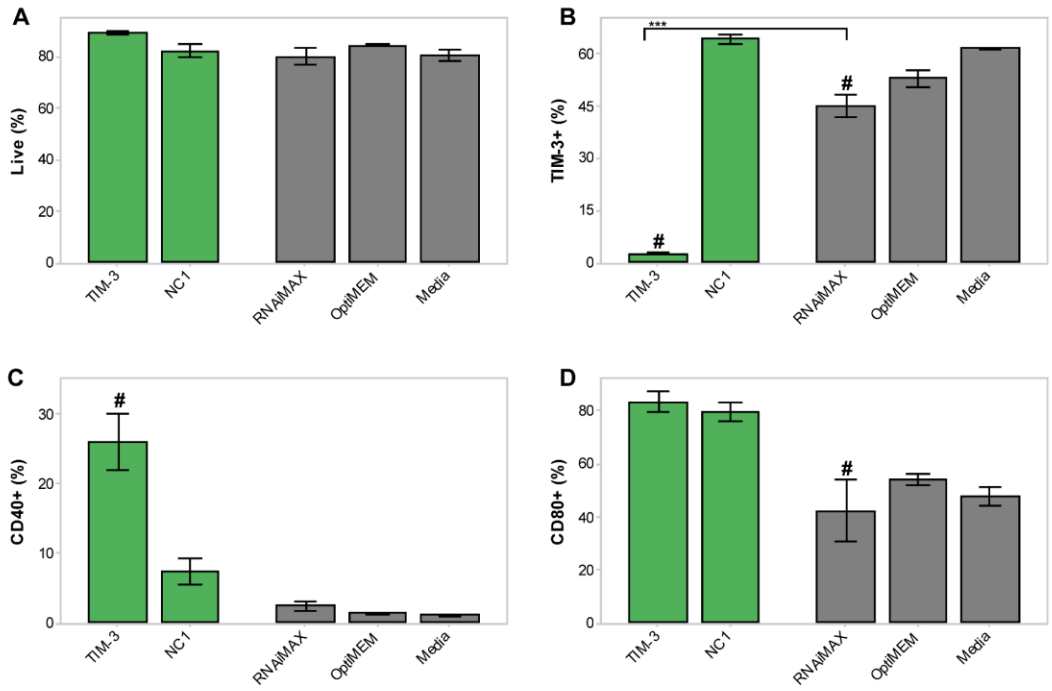

Figure 3.7 TIM-3 silencing with DsiRNA in RAW264.7 cells
RAW264.7 cells were transfected with TIM-3 targeted DsiRNA and NC1 DsiRNA at 10nM with Lipofectamine RNAiMAX and screened for viability (A, DAPI$^-$), TIM-3 expression (B), and co-stimulatory markers CD40 (C) and CD80 (D) by flow cytometry. Controls of RNAiMAX without any RNA, OptiMEM and media were also measured. Statistical symbols (p <0.05, **p<0.01, *** or # p<0.001) directly above individual bars indicate significant difference with NC1, while brackets indicate key relationships as labeled. Error bars: S.E.M.*

Upon reverse transfection at 10nM DsiRNA, RAW264.7 cells saw no change in viability for any condition, and we succeeded in drastically reducing TIM-3 expression

from ~60% to ~3% following a two day incubation (**Figure 3.7 A,B**). Moreover, a statistically significant increase in CD40 expression was detected among cells receiving the TIM-3 DsiRNA treatment (**Figure 3.7 C**); however, the increase observed in CD80 expression for both TIM-3 and NC1 DsiRNAs was not significant in comparison to media and vehicle controls (**Figure 3.7 D**).

3.4 Discussion

Our group's previous work with PBAEs using C57BL/6J mice *in vivo* and in primary DCs isolated from the same strain elicited stimulatory effects only when the PBAEs were formulated into particles[14,51]. First, we showed that PBAEs can be formulated into particles with both negative and positive charges (**Figure 3.1**) by varying w/w ratio of PBAE:RNA. At the extremes of the ratios for particle could be assembled, the complexes were smaller and more highly charged.

Next, we tested the soluble and complexed forms in RAW264.7 cells to see if we could increase maturation marker expression. Interestingly, our results here – in a different model from previous reports where PBAEs only activate in particle form[14,51] – suggest that PBAEs may act as an immunostimulatory adjuvant in *both* soluble and particle form. Given that RAW264.7 cells are derived from BALB/c mice, we cannot rule out possible immunological differences due to mouse strain[82,83]. Our findings are important because 1) new immunological adjuvant strategies are needed to enable more effective vaccines and immunotherapies and because 2) these types of pro-inflammatory effects should be taken into consideration when developing therapies

with PBAEs that might cause unwanted inflammation. Additionally, the intrinsic immunogenicity of polymers and other therapeutic delivery vehicles remains under studied, and the structure-function relationships of the most common clinically used adjuvants (e.g. alum) are still being established[10,11]. Although these findings should not be immediately extrapolated to all PBAEs, they should motivate investigations into the immunogenicity of the wide array of PBAEs already known to modulate cell interactions, transfection efficiency, and *in vivo* trafficking [49,50,84].

Although the PBAE used here clearly activated the RAW264.7 cells, our observations suggest that the effects are mechanistically distinct from the TLRa studied. LPS (TLR4a) induced a unique change in morphology (**Figure 3.4**) combined with much higher expression of CD40 (**Figure 3.3 A,B**) and more cell death (**Figure 3.3 G,H**) than PBAE and all other treatments and induced. This strong response to LPS including cell death is expected[62], but differs somewhat from primary DC cultures, which tend to have increased survival with similar LPS treatments[14,51]. In contrast, polyIC (TLR3a) showed no signs of activating the cells, while R848 (TLR7/8a) and PBAE induced moderate to high levels of activation on both CD80 and CD86 (**Figure 3.3 C-F**), nearing that of LPS without compromising viability (**Figure 3.3 G,H**). Furthermore, PBAE and polyIC were unable to induce IL-6 expression (**Figure 3.5**).

We hypothesized that the PBAE immunogenicity would be regulated through the IRF and/or NF-κB transcription factors due their broad roles in regulating many of the most common pro-inflammatory signaling pathways[74,75]. Intriguingly, PBAE showed no

sign of signaling through either IRF or NF-κB (**Figure 3.6**). Although this is only one means of measuring IRF and NF-κB induction, these preliminary results support the notion that PBAE is activating RAW264.7 cells by some means other than pathogen recognition receptors such as TLRs, which tend to signal through one or both of those transcription factors. It will be important to establish the inflammatory pathway activated by PBAE because different pathways have distinct functions in the context of disease. For example, macrophages can become activated when repairing tissue or resolving inflammation caused by wounds, and they can become activated in response to a pathogen or when effecting anti-tumor activity[54,64].

3.5 Ongoing and Future work

3.5.1 Isolating the mechanism for PBAE intrinsic immunogenicity

Additional work is required to confirm that PBAE is not activating RAW264.7 cells through IRF and NF-κB and to identify how maturation of these cells is occurring. Measurement of IL1-ß could show interaction of PBAE with the inflammasome, but may require priming with another TLRa due to NF-κB's role in IL1-ß secretion[85]. Alternatively, inflammasome activity might be regulated with an inhibitor such as glybenclamide to determine whether inhibition reduces PBAE activation by arresting K^+ efflux[86]. Another potential mechanism involves the complement receptor 3, CR3, which is expressed on RAW264.7 cells[62], and is involved in phagocytosis/opsonization of certain pathogens in a MyD88-indpendent manner, may preclude IRF and NF-κB[87].

3.5.2 Resolving the utility of different models

As mentioned above, immunological variation among mouse strains[83] and cell type (i.e. DCs versus macrophages) may explain some of the differences from this study in comparison to our lab's previous work. Additionally, because RAW264.7 cells are immortalized, they may further differ from data collected with primary cells. Additional *in vivo* investigations and *in* vitro experiments primary cell experiments mirroring previous work could elucidate whether these differences are primarily due to strain or due to the specific nature of RAW264.7 cells. Moreover, because distinctions from mouse to human immune systems also exist[88], the cataloging the changes across pre-clinical models is of considerable interest to abate the frequent failure to translate candidate therapies to clinical successes – fewer than 10% of pharmaceutical candidates make it from Phase I trials to approval, with success for oncology indications resting at 5.1% [89,90]. Experiments with *ex vivo* human cells could provide also be used for comparison to these mouse models as another indicator of clinical potential.

3.5.3 Synergy with functional nucleic acid delivery

Our preliminary model for screening effects of DsiRNA silencing of TIM-3 shows promise in regulating TIM-3 expression and modest effects on RAW264.7 activation. Given successful, tunable formulation of PBAE with DsiRNA, these formulations should be tested for efficacy in attenuating TIM-3 expression while simultaneously promoting further activation of these cells. Studies incorporating these complexes in tumor models (e.g. B16F10, EG7-OVA) via intratumoral or intra-lymph node delivery

could reveal further effects on other antigen presenting cells and lymphocytes by restoring their effector functions. Moreover, this platform is modular in that any DsiRNA could be substituted including other checkpoint molecules or genes that suppress pro-inflammatory responses in cancer. Finally, these complexes could be delivered alongside model (e.g. OVA) or tumor differentiation antigens (e.g. gp100, TRP2[91]) to assess whether they can promote antigen-specific effector functions.

Above, we detailed the results of our first aim in which we show that PBAEs activate RAW264.7 cells in soluble and particulate forms. In **Chapter 4** we use the same RAW264.7 model and a primary DCs (in which soluble PBAEs are not immunogenic[14,51]) to study this thesis's second aim: investigating the intrinsic immunogenicity of rationally designed RNA nanostructures in soluble form and in PBAE complexes for use as pro-inflammatory signals.

Chapter 4 : RNA nanostructures stimulate antigen presenting cells with and without a delivery vehicle

4.1 Introduction and motivating work

Therapeutic cancer vaccines that arm immune cells against antigens over-expressed on cancer cells have the potential to transform cancer therapy. However, these vaccines have been hindered by 1) inefficient expansion of T cells against tumor antigens, 2) an inability to maintain anti-tumor response in the immune-suppressive tumor microenvironment, and 3) poor generation of tumor-specific T cell memory to prevent relapse. More rational adjuvant design could address these challenges by activating robust sets of pro-immune pathways to drive potent, durable expansion of tumor-specific T cells.

Recent clinical trials show that activating pro-immune inflammatory toll-like receptors (TLRs) in cancer therapy allows the immune system to access and mount responses to tumor-associated antigens[92]. Several of these TLR pathways detect nucleic acid based signals (e.g. TLR3, dsRNA; TLR7, ssRNA; TLR9, CpG DNA) that occur in viral and bacterial pathogens. Recent studies in Dr. Bruce Shapiro's group have revealed complete control over the assembly of RNA-DNA, DNA-DNA, or RNA-RNA nanostructures (NS)[93–97]. Importantly, evidence of intrinsic immunogenic features of these structures were also observed, triggering modest levels of inflammatory cytokines[95,97]. Given these findings and the potential of RNA NS to trigger multiple

TLRs, we hypothesize these materials might create a new class of potent, rationally designed adjuvants.

Importantly, the kinetics and concentrations over which vaccine adjuvants are delivered play a major role in the magnitude of response.[98,99] Thus, our strategy incorporates a degradable cationic poly(β-amino ester) (PBAE) to investigate delivery via electrostatic assembly with the anionic RNA NS.

We selected these RNA NS because work published by Dr. Shapiro's group demonstrates complete control over the assembly of nucleic acid nanostructures. RNA NS that are computationally designed[100] have been successfully assembled *in vitro* with predictable size and shape verified by gel migration, dynamic light scattering (DLS), and electron microscopy [93–97,100–102]. The four RNA NS studied here – the nanoring, nanoring with arms, nanocube, and nanocube with arms – were not designed explicitly to promote immune function. Rather, these RNA NS were assembled as scaffolds for functional payloads such as aptamers, siRNAs, and fluorescent sensors. For example, two of the RNA NS that we are studying include siRNA "arms" that target enhanced green fluorescent protein (eGFP, an exogenous reporter protein not normally expressed in immune tissues), and these types of RNA NS have been shown to exhibit functional activity against eGFP [94,95,97]. Because exogenous RNAs can trigger pro-inflammatory responses, and initial studies with RNA NS delivered by lipofection triggered cytokine secretion under certain conditions[95,97], we hypothesized that these RNA NS may have intrinsic immunogenic properties.

Previous work by the Shapiro group used Lipofectamine 2000 (L2000, a commercial, lipid-based reagent for nucleic acid delivery in complexes) to deliver RNA NS to human peripheral blood mononuclear cells (PBMCs) in two separate studies. In the first study, L2000 delivery of RNA nanocubes and nanocubes with arms induced pro-inflammatory secretion of type I interferon (IFNß) and IL-1ß, whereas similar DNA-based nanostructures did not elicit the same level of cytokine secretion [95]. In the second study, cytokine secretion induced by nanostructures was measured in comparison to a synthetic CpG oligonucleotide (ODN 2216), a TLR9 agonist[97]. RNA nanocubes caused secretion of IL-1ß, IL-8, TNFα, and MIP-1α at consistently higher levels when compared to DNA nanocubes, and IL-8 and MIP-1α were secreted at levels similar to CpG.

We are motivated by these studies to understanding the intrinsic immunogenicity of RNA NS, which appear to be more potent modulators of immunity than similar constructs assembled from DNA. These properties could depend on content, shape, functionalization, among other parameters that are of interest to inform rational design of new vaccine adjuvants. Here, we investigate the ability of RNA NS to modulate immunity on their own, and we attempt to enhance RNA NS immunogenicity through complexation with a poly(ß-amino ester) to form nanoparticles. We utilize two *in vitro* mouse antigen presenting cell (APC) models: RAW264.7 cell line (immortalized mouse macrophages) and freshly isolated mouse dendritic cells (DCs). These APCs

recognize TLRa and are responsible for initiation pro-immune pathways. We hypothesize that these RNA NS and associated complexes will activate mouse APCs.

4.2 Methods

4.2.1 Materials

PBAE was synthesized in a Michael-type addition reaction using standard methods previously described[14]. Dulbecco's modified eagle medium (DMEM), Roswell Park Memorial Institute (RPMI) medium 1640, and fetal bovine serum (FBS) were purchased from Gibco, Lonza, and Corning, respectively. NC1 DsiRNA was synthesized by Integrated DNA Technologies and resuspended at 20µM in nuclease free water as a control.

4.2.2 Cells and mice

RAW264.7 cells were purchased from ATCC and maintained in DMEM containing 4.5g/l glucose and 4mM l-glutamine for no more than 10 passages. DMEM was supplemented with 10% FBS. Primary dendritic cell cultures were isolated from C57BL/6J mice using CD11c positive selection microbeads (Miltenyi). Primary DCs were cultured without passaging in RPMI 1640 containing 2mM l-glutamine and 25mM HEPES. RPMI was supplemented with 10% FBS and 55µM ß-mercaptoethanol and 1X penicillin streptomycin. All studies involving animals were conducted in compliance with federal, state, and local guidelines, and in accordance with the policies and review of the University of Maryland's Institutional Animal Care and Use Committee (IACUC).

4.2.3 RNA NS assembly

RNA NS were assembled from RNA monomer strands in solution (89mM Tris-borate, 2mM magnesium acetate, 50mM KCl) as described in previous work[96]. Briefly, DNA was purchased (Integrated DNA Technologies) and transcribed into RNAs *in vitro* from PCR-amplified template DNA using T7 RNA polymerase and purified on denaturing urea gels. Equimolar RNA monomer solutions were prepared, mixed, heated, and cooled per individual construct requirements in the one-pot assembly method[96]. Assembly was verified by running constructs on native PAGE gels to ensure visualization of a single band per NS.

4.2.4 Complex formulation

Complexes were produced by mixing solutions of PBAE and RNA NS in 25mM sodium acetate buffer (NaAc, pH 5). All buffer solutions for complex formation were filtered (0.2µm). Complexes were formed at varying w/w ratios while v/v was kept at a constant 1:1 with each solution added in 25µL volumes for 50µL total volume per batch. For cell studies, all complexes were formulated using 1:1 w/w mixtures. RNA NS were diluted to 40µg/mL for 1µg in 25µL NaAc, and PBAE solutions were serially diluted to vary the w/w ratio of a complex components following 0.2µm filtration of PBAE in solution at 2mg/mL and further dilution (40µg/mL for cell studies and variable concentrations for certain physiochemical studies). Complexes were mixed vigorously by pipetting and used immediately for either physiochemical

characterization or cell treatments. Control complexes were formulated in the same manner using NC1 DsiRNA.

4.2.5 Complex size and zeta potential measurements

Dynamic light scattering (DLS, size) and electrophoretic light scattering (ELS, zeta potential) were performed using a Malvern Zetasizer Nano ZS90. Measurements were made in disposable 50µL cuvettes and zeta potential capillary cells for DLS and ELS, respectively. All measurements were conducted in 0.2µm filtered 25mM sodium acetate buffer.

4.2.6 Quantification of immune stimulation by flow cytometry

Complexes and soluble treatments were prepared to be plated in triplicate at 25µl/well (500ng RNA NS and/or PBAE per well). Activation experiments took place with RAW264.7 cells and primary DCs in the same manner other than cell harvesting/isolation and culture mediaRAW264.7 cells were passaged (no greater than P10) by cell scraping, while $CD11c^+$ splenic dendritic cells were freshly isolated. . Single cell suspensions were seeded at ~55,000 cells per well in 175µL for a total culture volume of 200µl over the prepared treatments (i.e. complexes, soluble polymer or RNA, TLRa, and buffer/media controls). DCs were collected after overnight incubation, while RAW264.7 cells were collected after two nights. After blocking the Fc receptors, cells were stained with fluorescent antibodies for surface activation markers (i.e. CD40, CD80, CD86, IA-IE (DCs only)) and with a viability dye (DAPI).

Flow cytometry (BD FACSCanto II) was used to determine relative levels of activation through analysis using FlowJo (v.10.2, TreeStar, Ashland, OR).

4.2.7 Statistical analysis

Multiple pairwise comparisons were performed using the Tukey method in Minitab 17 with a p-value less than 0.05 indicating significance. All error bars are reported as standard error of the mean (S.E.M.) unless stated otherwise.

4.3 Results

4.3.1 Free RNA NS induce baseline activation of dendritic cells

In an initial study, we measured the baseline immunogenicity of nanocubes and nanorings. We tested if free RNA NS exhibited intrinsic immunostimulatory properties by treating $CD11c^+$ dendritic cells (DCs) isolated from mouse spleens with RNA NS over a range of concentrations. The free RNA NS do not affect viability in comparison to a vehicle buffer control (**Figure 4.1 A**). DC activation levels for one set of concentrations (50nM) is indicated by the relative increases in CD86 (**Figure 4.1 B**) and CD80 (**Figure 4.1 C**) in comparison to a strong nucleic acid adjuvant (polyIC, TLR3a) as a positive control. These baseline measurements suggest that these RNA NS are intrinsically immunogenic and that their immunogenicity may be enhanced through alternative dosing or delivery strategies. This finding motivated formulation of RNA NS with PBAE and further study of both free and complexed RNA NS (**Figure 4.2 B**). Further studies below delivered RNA NS at constant mass (rather than molar)

quantities to avoid complications in study design when delivering free and complexed RNA NS.

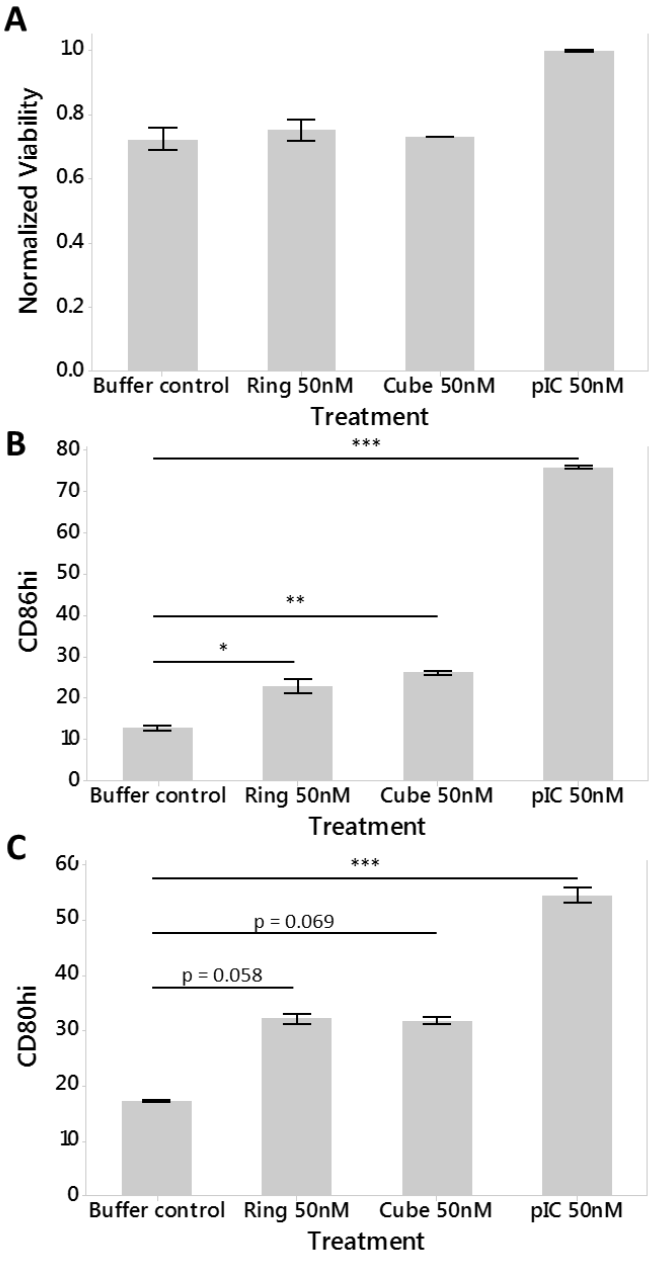

Figure 4.1 Baseline immunogenicity of RNA NS
*CD11c^{+} splenic DCs treated with free RNA NS, buffer control, and polyIC (pIC) analyzed by flow cytometry for viability (A) and baseline percent of high expression of markers CD86 (B) and CD80 (C) among live, single cells. Viability normalized to polyIC control. Error bars: S.E.M.; *p < 0.05; **p < 0.01; ***p < 0.001*

4.3.2 PBAE and RNA NS assemble into charged nanoparticles

RNA NS and PBAE were mixed and assembled via electrostatic assembly in 25mM sodium acetate. The complex charge and size were tunable based on the w/w ratio of PBAE:RNA (**Figure 4.2 C,D**) with more highly charged particles tending to have smaller diameters. We also assembled complexes from NC1 DsiRNA, which was selected to be used as an additional control because it does not target any known sequence in the mouse transcriptome, and because it is a linear duplex rather than a complex nanostructure. To minimize effects of PBAE in cell studies, we selected the 1:1 w/w ratio so that we would be able to deliver sufficient mass of RNA NS to observe an effect while staying well below the toxicity threshold of PBAE. When measured immediately following assembly, complexes formed below 500nm in all cases (**Table 4.1**).

Table 4.1 Mean diameters and polydispersity of complexes
Means of at least two separate experiments are reported for Z-average diameter and polydispersity index (PDI) of 1:1 w/w complexes with RNA NS and NC1 DsiRNA measured by DLS.

RNA Type:	**Ring**	**Ring + arms**	**Cube**	**Cube + arms**	**NC1**
Mean Z-avg diameter (nm)	316	407	359	384	243
Mean PDI	0.070	0.148	0.144	0.076	0.078

4.3.3 Complexes and free RNA NS or PBAE activate RAW264.7 cells

Our first set of studies with complexed RNA NS use RAW264.7 cells, delivered at a fixed mass dose of RNA NS (2.5µg/mL). Because complexes were assembled at 1:1 w/w ratio, complex treatments contained PBAE at that same volume. We used flow cytometry to compare RAW264.7 maturation markers (CD40, CD80, and CD86)

among live cells treated with free or complexed RNA NS to controls including a matched dose of free PBAE and a positive control (LPS). No treatment group exhibited viability lower than PBAE or LPS treated cells (**Figure 4.3 A**). For all maturation markers (**Figure 4.3 B-D**), the PBAE soluble control activated RAW264.7 cells above the media and buffer controls, but lower than the LPS controls (as expected and discussed in **Chapter 3 above**).

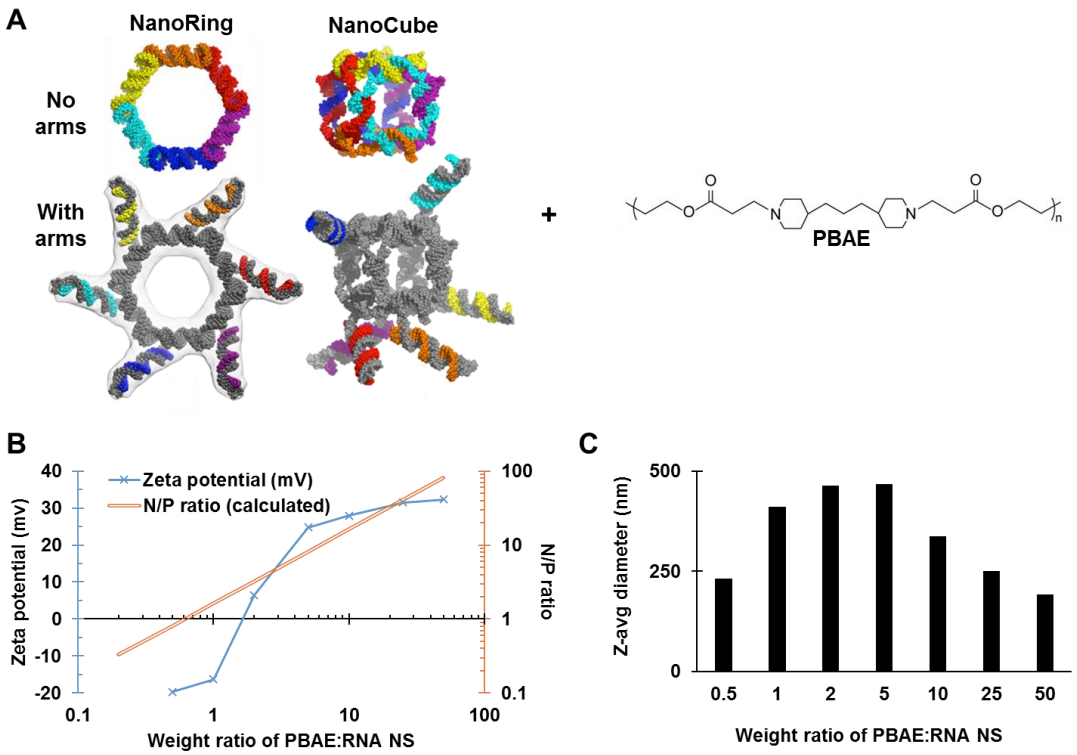

Figure 4.2 Structure of RNA NS and PBAE with representative complex charge and diameter. RNA NS structures were assembled into complexes with PBAE (A) at varying w/w ratios. Charge (B) and size (C) of the resultant complexes was measured (data for Nanoring w/ arms shown). Predicted N/P ratio was calculated and is shown alongside measured particle charge (B).

All complexed RNA NS increased levels of CD80 and CD86 expression compared to buffer controls (**Figure 4.3 C,D**). Soluble nanoring and nanocube exhibited statistically higher levels of CD80 expression than media and buffer controls (**Figure 4.3 C**),

whereas only the nanoring was the only soluble RNA NS able to upregulate expression of CD86 under these conditions (**Figure 4.3 C,D**). RNA NS did not appear to affect CD40 expression in comparison to equivalent soluble controls (**Figure 4.3 B**).

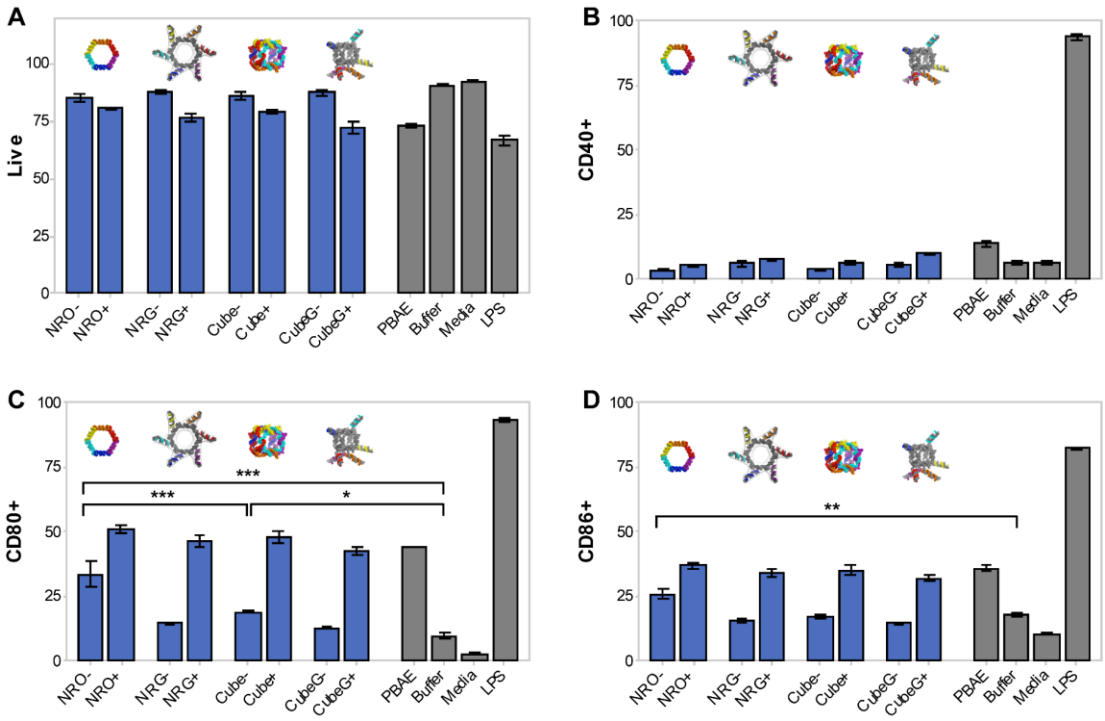

Figure 4.3 RAW264.7 cell activation by RNA NS and complexes
RNA NS delivered soluble without (-) and complexed with (+) PBAE at 2.5µg RNA/mL. Percent viability (A) and of maturation marker expression (B:CD40$^+$, C:CD80$^+$, D:CD86$^+$) among live cells was assessed by flow cytometry. Nanoring (NRO), nanoring with anti-eGFP arms (NRG), cube, and cube with anti-eGFP arms (CubeG) in blue. Controls in gray. All samples in triplicate. For clarity, only key statistical comparisons for maturation markers are shown (p <0.05, **p<0.01, *** p<0.001) as indicated by brackets between individual soluble (-) treatments. No complexed treatments (+) induced more maturation than the soluble PBAE control. Error bars: S.E.M.*

4.3.4 Complexes and free RNA NS activate primary DCs

Our experiments with RAW264.7 cells enabled us to set up a similar set of experiments in primary DCs with an additional set of control treatments; the NC1 DsiRNA was chosen and delivered as a soluble or complexed double-stranded RNA control because it does not target any known part of the mouse transcriptome, nor does it form nanostructures on its own. DCs were treated and assessed in the same manner as the

RAW264.7 cells. As expected, soluble PBAE alone did not activate primary C57BL/6J DCs[14,51], no groups experienced viability lower than their equivalent vehicle control groups (buffer or PBAE, **Figure 4.4 A**), and all groups had high (>90%) expression of MHCII (not shown).

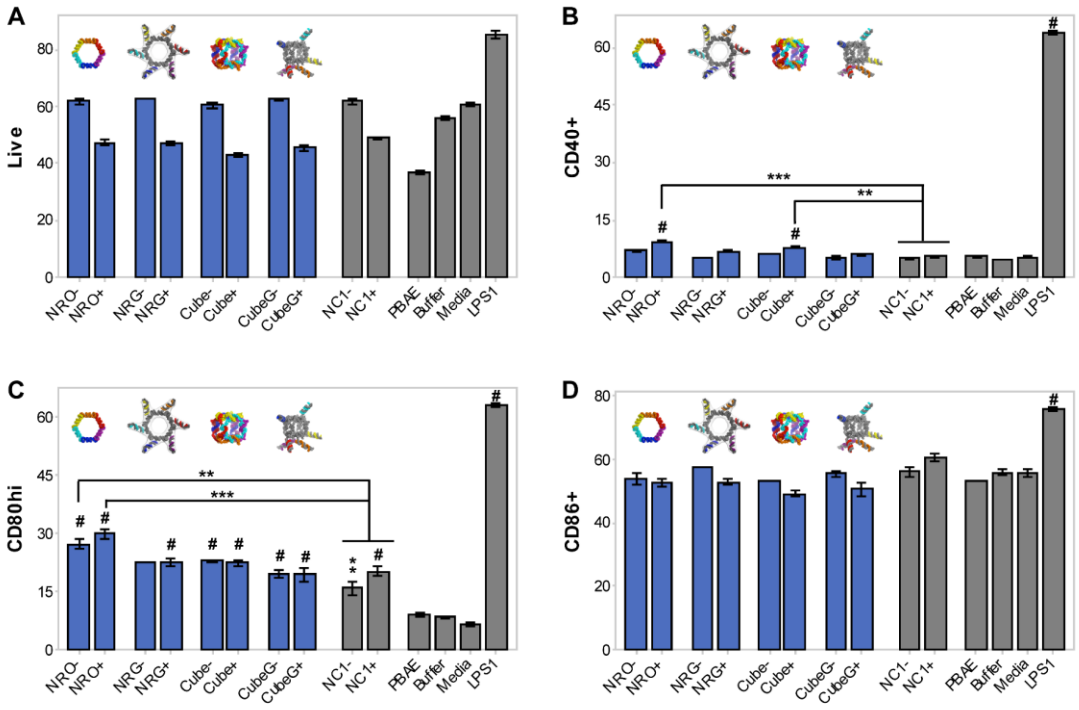

Figure 4.4 Dendritic cell activation by free and complexed RNA NS
RNA NS delivered without (-) and complexed with (+) PBAE at 2.5μg RNA/mL. Percent viability (A) and of maturation marker expression (B:CD40$^+$, C:CD80hi, D:CD86$^+$) among live cells was assessed by flow cytometry. Nanoring (NRO), nanoring with anti-eGFP arms (NRG), cube, and cube with anti-eGFP arms (CubeG) in blue. Controls in gray. All samples in triplicate except single sample of NRG-. For maturation markers, statistical symbols (p <0.05, **p<0.01, *** or # p<0.001) directly above individual bars indicate significance against all three (PBAE, buffer, and media) vehicle controls. Brackets show significance against both NC1 controls. Error bars: S.E.M.*

Only the complexed nanocube and nanoring were able to induce modest, statistically significant increases in CD40 expression (**Figure 4.4 B**). All RNA-containing treatments and controls (soluble and complexed) induced upregulation of CD80 in comparison to PBAE and buffer/media controls (**Figure 4.4 C**); however, the only set

of RNA NS treatments to exceed both NC1 controls for CD80 was the nanoring group – both soluble and complexed forms exceeded soluble and complexed NC1 CD80 expression. Finally, no RNA NS exceeded NC1 or PBAE/buffer/media controls in CD86 expression (**Figure 4.4 D**).

4.4 Discussion and future work

4.4.1 Discussion

Motivated by previous findings that RNA NS elicited cytokine secretion in human PBMCs when delivered by lipofection[95,97], we sought to answer two questions: 1) what is the nature of RNA NS intrinsic immunogenicity and 2) can we enhance/control RNA NS immunogenicity by formulating them with PBAE. In our initial study, we found that RNA NS delivered to primary mouse DCs at 50nM exhibited modest levels of increases to DC maturation markers (**Figure 4.1**). In subsequent experiments with RAW264.7 cells and primary DCs, we used smaller, fixed-mass doses (13-31nM, depending on RNA NS structure), so that we could assemble similar, non-toxic particles with PBAE (**Figure 4.2**).

Even at these lower soluble doses, we saw that soluble delivery of the nanoring and the nanocube exhibited increased activity in RAW264.7 cells (**Figure 4.3 C,D**), whereas the same structures with arms did not appear to induce additional maturation in soluble form. Moreover, all RNA NS were able to stimulate RAW264.7 cells when complexed with PBAE, but no treatment exceeded soluble PBAE potency, which can likely be accounted for through PBAE's intrinsic immunogenicity in RAW264.7 cells explored in greater detail in **Chapter 3 above**.

In contrast, PBAE alone did not induce primary C57Bl/6J DC maturation, as expected from our lab's prior studies in this model[14,51]. In all RNA-containing treatments increased CD80 expression in primary DC culture when compared to negative controls without RNA (**Figure 4.4 C**). In this model, the nanoring performed better than other RNA NS, exceeding NC1 DsiRNA controls' potential in both soluble and complexed form to increase CD80 expression. Additionally, the nanoring and cube, when complexed, were the only RNA NS to affect CD40 expression, causing modest increases (**Figure 4.4 B**). Taken together, observations in both models suggest that certain RNA NS – the nanoring without arms in particular – exhibit intrinsic immune effects that may be enhanced by PBAE complexation. Future studies, some of which are highlighted below, could provide greater support for RNA NS intrinsic immunogenicity in mouse APCs.

4.4.2 Assessing synthesis and stability limitations with additional physiochemical characterization

Building on the measurements above, we can complete the physiochemical analyses to understand any benefits of PBAE-complexed RNA NS. A nucleic acid intercalator (e.g. SYBR) exclusion assay can be used to measure the affinity between the RNA NS and PBAEs as a function of N/P ratio. Size and zeta potential measurements before and after incubation with physiologic media/buffer and enzymes (e.g. RNAse) over time could provide insight into the stability and protective capacity of the complexes, which may correlate with their ability to act successfully as adjuvants. Following similar incubations, we can assess complex ability to protect the RNA NS from degradation

using gel migration assays. Electron microscopy at select PBAE:RNA NS ratios could also be used to validate DLS size measurements and reveal the nature of the PBAE-RNA NS complex morphology. This insight could improve our understanding of future size/shape-dependent uptake in the studies in APCs described below.

4.4.3 Understanding mechanism of immune interaction and specificity by cell type and pathway

Although our studies in these two APC models revealed some activation, it is unclear whether the mechanisms involved are as potent in mouse cells as those previously reported in human samples [95,97]. Further mechanistic studies could reveal whether we see similar cytokine secretion, and could be used to verify whether there are any mouse strain or human/mouse species differences [83,88]. For example, APCs (DCs and/or macrophages) could be isolated from the spleens of C57BL/6J and BALB/c mice and be incubated with labeled PBAE-RNA NS complexes or soluble controls to measure adjuvant uptake/association and cell viability (with DAPI) by confocal microscopy and flow cytometry. Because most nucleic TLRa act in the endosome, uptake of these NS might be correlated with potency[43]. Similar studies could compare the ability of each structure to activate DCs in free and PBAE-complexed forms by quantifying expression of CD40, CD80, CD86, and MHC-II by flow cytometry and production of inflammatory cytokines including IL-1β, IFN-γ, IL-8, TNFα, and MIP-1α by ELISA. These results could be used to infer whether the RNA NS act in mouse cells similarly to the previous reports, which relied solely on cytokine measurements as an indicator of immunogenicity.

In a second type of study, model peptide antigen (SIINFEKL) could be added to each well of C57BL/6J cells to test if RNA NS drive increased antigen presentation, measured using an antibody that binds the SIINFEKL epitope when presented in the MHC-I complex – a pathway important in cytotoxic T cell responses. Further, we could determine if each adjuvant formulation expands tumor-specific T cells by treating DCs with each structure for 24 hours, along with a well-studied melanoma peptide antigen (gp100 or TRP2) and initiating a co-culture with splenic $CD8^+$ T cells from Pmel-1 or TRP-2 mice, respectively for 72 hrs. T cell receptors on $CD8^+$ T cells from the Pmel-1 and TRP-2 strains recognize gp100 and TRP2 presented in MHC-I by activated DCs causing proliferation[103,104]. Moreover, the most effective treatments identified by these experiments could then be used in similar mouse cancer models.

For example, initial *in vivo* studies might involve immunizing mice subcutaneously at the tail base on day 0 with a booster immunization on day 14 using a vaccine formulation containing both complexed RNA NS and one of the tumor antigens mentioned above. Weekly collection of peripheral blood could be screened using a MHC tetramer flow cytometry assay to identify antigen-specific $CD8^+$ T cell expansion against the model antigen. Treatments that work best to stimulate antigen-specific responses and other advantageous phenotypes (e.g. T_H17, T_H1) would then be used as treatments against tumor models such as EG7 thymoma. Treatments in this model could also examine whether vaccination containing RNA NS without exogenous antigen (i.e. not delivering EG7's dominant antigen (OVA)) might successfully activate immunity against tumor antigens that drain to lymph nodes [105–107].

A third type of study could use flow cytometry with donated human samples to assess maturation markers on human APCs and cytokine production by intracellular cytokine staining or ELISAs on cell supernatants.

4.4.4 Modulating functional immunogenicity or bioactivity within nanostructures by design

As mentioned in the introduction, the design of the RNA NS investigated in these studies was not carried out specifically to induce or avoid immunogenicity. Currently, the nanoring and nanocube are used as scaffolds for eGFP targeted siRNAs in the RNA NS with arms; however, in some cases, eGFP siRNAs may exhibit off-target effects due to sequence homology with other parts of the transcriptome[108]. Consequently, future work to isolate effects of these moieties and explore only the relationship of RNA NS size/shape dependence could be carried out by replacing the arms with an alternative structure such as the NC1 DsiRNA. Further, these NS could be designed to be functionalized specifically with known densities of TLRa structures like CpG ODN and polyIC, or with their antagonists (e.g. GpG ODN, which downregulates TLR9 activity despite similarities to CpG structure [109]). In this manner, one could specifically investigate potency of these structures and modulate the density of the signals displayed through combinations or different numbers of these signals in place of the arms on the RNA NS scaffolds.

References

[1] Organization, W. H. Polio this week as of 24 May 2017 http://polioeradication.org/polio-today/polio-now/this-week/ (accessed May 29, 2017).

[2] Gammon, J. M.; Dold, N. M.; Jewell, C. M. Improving the Clinical Impact of Biomaterials in Cancer Immunotherapy. *Oncotarget* **2016**, *7*, 15421–15443.

[3] Tostanoski, L. H.; Gosselin, E. A.; Jewell, C. M. Engineering Tolerance Using Biomaterials to Target and Control Antigen Presenting Cells. *Discov. Med.* **2016**, *21*, 403–410.

[4] Kelly, S. H.; Shores, L. S.; Votaw, N. L.; Collier, J. H. Biomaterials Strategies for Generating Therapeutic Immune Responses. *Adv. Drug Deliv. Rev.* **2017**.

[5] Scott, E. A.; Karabin, N. B.; Augsornworawat, P. Overcoming Immune Dysregulation with Immunoengineered Nanobiomaterials. *Annu. Rev. Biomed. Eng.* **2017**, *19*, annurev-bioeng-071516-044603.

[6] Pearson, R. M.; Casey, L. M.; Hughes, K. R.; Miller, S. D.; Shea, L. D. In Vivo Reprogramming of Immune Cells: Technologies for Induction of Antigen-Specific Tolerance. *Adv. Drug Deliv. Rev.* **2017**.

[7] Abbas Abul K.; Lichtman;, A. H.; Pillai, S. *Cellular and Molecular Immunology*; 2014; Vol. 8ª ed.

[8] Iwasaki, A.; Medzhitov, R. Control of Adaptive Immunity by the Innate Immune System. *Nat. Immunol.* **2015**, *16*, 343–353.

[9] Levy, M.; Kolodziejczyk, A. A.; Thaiss, C. A.; Elinav, E. Dysbiosis and the Immune System. *Nat. Rev. Immunol.* **2017**, *17*, 219–232.

[10] O'Hagan, D. T.; Fox, C. B. New Generation Adjuvants--from Empiricism to Rational Design. *Vaccine* **2015**, *33 Suppl 2*, B14-20.

[11] Mold, M.; Shardlow, E.; Exley, C. Insight into the Cellular Fate and Toxicity of Aluminium Adjuvants Used in Clinically Approved Human Vaccinations. *Sci. Rep.* **2016**, *6*, 31578.

[12] Sharp, F. a; Ruane, D.; Claass, B.; Creagh, E.; Harris, J.; Malyala, P.; Singh, M.; O'Hagan, D. T.; Pétrilli, V.; Tschopp, J.; *et al.* Uptake of Particulate Vaccine Adjuvants by Dendritic Cells Activates the NALP3 Inflammasome. *Proc. Natl. Acad. Sci. U. S. A.* **2009**, *106*, 870–875.

[13] Torres, M. P.; Wilson-Welder, J. H.; Lopac, S. K.; Phanse, Y.; Carrillo-Conde, B.; Ramer-Tait, A. E.; Bellaire, B. H.; Wannemuehler, M. J.; Narasimhan, B. Polyanhydride Microparticles Enhance Dendritic Cell Antigen Presentation and Activation. *Acta Biomater.* **2011**, *7*, 2857–2864.

[14] Andorko, J. I.; Hess, K. L.; Pineault, K. G.; Jewell, C. M. Intrinsic Immunogenicity of Rapidly-Degradable Polymers Evolves during Degradation. *Acta Biomater.* **2015**, *32*, 24–34.

[15] Tzeng, S. Y.; Guarecuco, R.; McHugh, K. J.; Rose, S.; Rosenberg, E. M.; Zeng, Y.; Langer, R.; Jaklenec, A. Thermostabilization of Inactivated Polio Vaccine in PLGA-Based Microspheres for Pulsatile Release. *J. Control. Release* **2016**, *233*, 101–113.

[16] Wang, F.; Fang, R. H.; Luk, B. T.; Hu, C.-M. J.; Thamphiwatana, S.; Dehaini, D.; Angsantikul, P.; Kroll, A. V.; Pang, Z.; Gao, W.; *et al.* Nanoparticle-Based Antivirulence Vaccine for the Management of Methicillin-Resistant

Staphylococcus Aureus Skin Infection. *Adv. Funct. Mater.* **2016**, *26*, 1628–1635.

[17] Yeste, a.; Nadeau, M.; Burns, E. J.; Weiner, H. L.; Quintana, F. J. Nanoparticle-Mediated Codelivery of Myelin Antigen and a Tolerogenic Small Molecule Suppresses Experimental Autoimmune Encephalomyelitis. *Proc. Natl. Acad. Sci.* **2012**, *109*, 11270–11275.

[18] Maldonado, R. A.; LaMothe, R. A.; Ferrari, J. D.; Zhang, A.-H.; Rossi, R. J.; Kolte, P. N.; Griset, A. P.; O'Neil, C.; Altreuter, D. H.; Browning, E.; *et al.* Polymeric Synthetic Nanoparticles for the Induction of Antigen-Specific Immunological Tolerance. *Proc. Natl. Acad. Sci. U. S. A.* **2015**, *112*, E156-65.

[19] Tostanoski, L. H.; Chiu, Y. C.; Gammon, J. M.; Simon, T.; Andorko, J. I.; Bromberg, J. S.; Jewell, C. M. Reprogramming the Local Lymph Node Microenvironment Promotes Tolerance That Is Systemic and Antigen Specific. *Cell Rep.* **2016**, *16*, 2940–2952.

[20] Getts, D. R.; Martin, A. J.; McCarthy, D. P.; Terry, R. L.; Hunter, Z. N.; Yap, W. T.; Getts, M. T.; Pleiss, M.; Luo, X.; King, N. J. C.; *et al.* Microparticles Bearing Encephalitogenic Peptides Induce T-Cell Tolerance and Ameliorate Experimental Autoimmune Encephalomyelitis. *Nat. Biotechnol.* **2012**, *30*, 1217–1224.

[21] Kontos, S.; Kourtis, I. C.; Dane, K. Y.; Hubbell, J. A. Engineering Antigens for in Situ Erythrocyte Binding Induces T-Cell Deletion. *Proc. Natl. Acad. Sci. U. S. A.* **2013**, *110*, E60-8.

[22] Hess, K. L.; Oh, E.; Tostanoski, L. H.; Andorko, J. I.; Susumu, K.; Deschamps, J. R.; Medintz, I. L.; Jewell, C. M. Engineering Immunological Tolerance Using

Quantum Dots to Tune the Density of Self-Antigen Display. *Adv. Funct. Mater.* **2017**, *1700290*.

[23] Pishesha, N.; Bilate, A. M.; Wibowo, M. C.; Li, Z.; Dhesycka, R.; Bousbaine, D.; Lodish, H. F.; Ploegh, H. L.; Pishesha, N.; Bilate, A. M.; *et al.* Correction for Pishesha et Al., Engineered Erythrocytes Covalently Linked to Antigenic Peptides Can Protect against Autoimmune Disease. *Proc. Natl. Acad. Sci.* **2017**, *114*, E3583–E3583.

[24] Clemente-Casares, X.; Blanco, J.; Ambalavanan, P.; Yamanouchi, J.; Singha, S.; Fandos, C.; Tsai, S.; Wang, J.; Garabatos, N.; Izquierdo, C.; *et al.* Expanding Antigen-Specific Regulatory Networks to Treat Autoimmunity. *Nature* **2016**, *530*, 434–440.

[25] Singha, S.; Shao, K.; Yang, Y.; Clemente-Casares, X.; Solé, P.; Clemente, A.; Blanco, J.; Dai, Q.; Song, F.; Liu, S. W.; *et al.* Peptide–MHC-Based Nanomedicines for Autoimmunity Function as T-Cell Receptor Microclustering Devices. *Nat. Nanotechnol.* **2017**.

[26] Kuai, R.; Ochyl, L. J.; Bahjat, K. S.; Schwendeman, A.; Moon, J. J. Designer Vaccine Nanodiscs for Personalized Cancer Immunotherapy. *Nat. Mater.* **2016**, *16*, 489–496.

[27] Sadtler, K.; Estrellas, K.; Allen, B. W.; Wolf, M. T.; Fan, H.; Tam, A. J.; Patel, C. H.; Luber, B. S.; Wang, H.; Wagner, K. R.; *et al.* Developing a pro-Regenerative Biomaterial Scaffold Microenvironment Requires T Helper 2 Cells. *Science (80-.).* **2016**, *352*, 366–370.

[28] Doloff, J. C.; Veiseh, O.; Vegas, A. J.; Tam, H. H.; Farah, S.; Ma, M.; Li, J.;

Bader, A.; Chiu, A.; Sadraei, A.; *et al.* Colony Stimulating Factor-1 Receptor Is a Central Component of the Foreign Body Response to Biomaterial Implants in Rodents and Non-Human Primates. *Nat. Mater.* **2017**, *16*, 671–680.

[29] Ali, O. a; Huebsch, N.; Cao, L.; Dranoff, G.; Mooney, D. J. Infection-Mimicking Materials to Program Dendritic Cells in Situ. *Nat. Mater.* **2009**, *8*, 151–158.

[30] Kim, J.; Li, W. A.; Choi, Y.; Lewin, S. A.; Verbeke, C. S.; Dranoff, G.; Mooney, D. J. Injectable, Spontaneously Assembling, Inorganic Scaffolds Modulate Immune Cells in Vivo and Increase Vaccine Efficacy. *Nat. Biotechnol.* **2014**, *33*, 64–72.

[31] Stephan, S. B.; Taber, A. M.; Jileaeva, I.; Pegues, E. P.; Sentman, C. L.; Stephan, M. T. Biopolymer Implants Enhance the Efficacy of Adoptive T-Cell Therapy. *Nat. Biotechnol.* **2014**, *33*, 97–101.

[32] Liu, J. M. H.; Zhang, J.; Zhang, X.; Hlavaty, K. A.; Ricci, C. F.; Leonard, J. N.; Shea, L. D.; Gower, R. M. Transforming Growth Factor-Beta 1 Delivery from Microporous Scaffolds Decreases Inflammation Post-Implant and Enhances Function of Transplanted Islets. *Biomaterials* **2016**, *80*, 11–19.

[33] Rouphael, N. G.; Paine, M.; Mosley, R.; Henry, S.; McAllister, D. V; Kalluri, H.; Pewin, W.; Frew, P. M.; Yu, T.; Thornburg, N. J.; *et al.* The Safety, Immunogenicity, and Acceptability of Inactivated Influenza Vaccine Delivered by Microneedle Patch (TIV-MNP 2015): A Randomised, Partly Blinded, Placebo-Controlled, Phase 1 Trial. *Lancet* **2017**, *6736*, 1–10.

[34] DeMuth, P. C.; Min, Y.; Huang, B.; Kramer, J. a; Miller, A. D.; Barouch, D. H.; Hammond, P. T.; Irvine, D. J. Polymer Multilayer Tattooing for Enhanced

DNA Vaccination. *Nat. Mater.* **2013**, *12*, 367–376.

[35] Wang, C.; Ye, Y.; Hochu, G. M.; Sadeghifar, H.; Gu, Z. Enhanced Cancer Immunotherapy by Microneedle Patch-Assisted Delivery of Anti-PD1 Antibody. *Nano Lett.* **2016**, *16*, 2334–2340.

[36] Zeng, Q.; Gammon, J. M.; Tostanoski, L. H.; Chiu, Y. C.; Jewell, C. M. In Vivo Expansion of Melanoma-Specific T Cells Using Microneedle Arrays Coated with Immune-Polyelectrolyte Multilayers. *ACS Biomater. Sci. Eng.* **2017**, *3*, 195–205.

[37] Chiu, Y.-C.; Gammon, J. M.; Andorko, J. I.; Tostanoski, L. H.; Jewell, C. M. Modular Vaccine Design Using Carrier-Free Capsules Assembled from Polyionic Immune Signals. *ACS Biomater. Sci. Eng.* **2015**, *1*, 1200–1205.

[38] Tostanoski, L. H.; Chiu, Y. C.; Andorko, J. I.; Guo, M.; Zeng, X.; Zhang, P.; Royal, W.; Jewell, C. M. Design of Polyelectrolyte Multilayers to Promote Immunological Tolerance. *ACS Nano* **2016**, *10*, 9334–9345.

[39] Yin, Z.; Comellas-Aragones, M.; Chowdhury, S.; Bentley, P.; Kaczanowska, K.; Benmohamed, L.; Gildersleeve, J. C.; Finn, M. G.; Huang, X. Boosting Immunity to Small Tumor-Associated Carbohydrates with Bacteriophage Qβ Capsids. *ACS Chem. Biol.* **2013**, *8*, 1253–1262.

[40] Jobsri, J.; Allen, A.; Rajagopal, D.; Shipton, M.; Kanyuka, K.; Lomonossoff, G. P.; Ottensmeier, C.; Diebold, S. S.; Stevenson, F. K.; Savelyeva, N. Plant Virus Particles Carrying Tumour Antigen Activate TLR7 and Induce High Levels of Protective Antibody. *PLoS One* **2015**, *10*, 1–16.

[41] Sun, Z. Y.; Chen, P. G.; Liu, Y. F.; Zhang, B. D.; Wu, J. J.; Chen, Y. X.; Zhao,

Y. F.; Li, Y. M. Multi-Component Self-Assembled Anti-Tumor Nano-Vaccines Based on MUC1 Glycopeptides. *Chem. Commun.* **2016**, *52*, 7572–7575.

[42] Hudalla, G. A.; Sun, T.; Gasiorowski, J. Z.; Han, H.; Tian, Y. F.; Chong, A. S.; Collier, J. H. Gradated Assembly of Multiple Proteins into Supramolecular Nanomaterials. *Nat. Mater.* **2014**, *13*, 829–836.

[43] O'Neill, L. A. J.; Golenbock, D.; Bowie, A. G. The History of Toll-like Receptors - Redefining Innate Immunity. *Nat. Rev. Immunol.* **2013**, *13*, 453–460.

[44] Zhang, M.; Hong, Y.; Chen, W.; Wang, C. Polymers for DNA Vaccine Delivery. *ACS Biomater. Sci. Eng.* **2017**, *3*, 108–125.

[45] Akinc, A.; Anderson, D. G.; Lynn, D. M.; Langer, R. Synthesis of Poly(beta-Amino Ester)s Optimized for Highly Effective Gene Delivery. *Bioconjug. Chem.* **2003**, *14*, 979–988.

[46] Tang, D.; Kang, R.; Coyne, C. B.; Zeh, H. J.; Lotze, M. T. PAMPs and DAMPs: Signal 0s That Spur Autophagy and Immunity. *Immunol. Rev.* **2012**, *249*, 158–175.

[47] Lynn, D. M.; Langer, R. Degradable Poly(β-Amino Esters): Synthesis, Characterization, and Self-Assembly with Plasmid DNA. *J. Am. Chem. Soc.* **2000**, *122*, 10761–10768.

[48] Anderson, D. G.; Lynn, D. M.; Langer, R. Semi-Automated Synthesis and Screening of a Large Library of Degradable Cationic Polymers for Gene Delivery. *Angew. Chemie - Int. Ed.* **2003**, *42*, 3153–3158.

[49] Kim, J.; Sunshine, J. C.; Green, J. J. Differential Polymer Structure Tunes

Mechanism of Cellular Uptake and Transfection Routes of Poly(β-Amino Ester) Polyplexes in Human Breast Cancer Cells. *Bioconjug. Chem.* **2014**, *25*, 43–51.

[50] Sunshine, J. C.; Peng, D. Y.; Green, J. J. Uptake and Transfection with Polymeric Nanoparticles Are Dependent on Polymer End-Group Structure, but Largely Independent of Nanoparticle Physical and Chemical Properties. *Mol. Pharm.* **2012**, *9*, 3375–3383.

[51] Andorko, J. I.; Pineault, K. G.; Jewell, C. M. Impact of Molecular Weight on the Intrinsic Immunogenic Activity of Poly(beta Amino Esters). *J. Biomed. Mater. Res. - Part A* **2017**, *105*, 1219–1229.

[52] Jackson, A. L.; Linsley, P. S. Recognizing and Avoiding siRNA off-Target Effects for Target Identification and Therapeutic Application. *Nat. Rev. Drug Discov.* **2010**, *9*, 57–67.

[53] Ku, S. H.; Jo, S. D.; Lee, Y. K.; Kim, K.; Kim, S. H. Chemical and Structural Modifications of RNAi Therapeutics. *Adv. Drug Deliv. Rev.* **2015**, *104*, 16–28.

[54] Jakubzick, C. V.; Randolph, G. J.; Henson, P. M. Monocyte Differentiation and Antigen-Presenting Functions. *Nat. Rev. Immunol.* **2017**.

[55] Zhang, J.; Saltzman, M. Engineering Biodegradable Nanoparticles for Drug and Gene Delivery. *Chem. Eng. Prog.* **2013**, *109*, 25–30.

[56] Gause, K. T.; Wheatley, A. K.; Cui, J.; Yan, Y.; Kent, S. J.; Caruso, F. Immunological Principles Guiding the Rational Design of Particles for Vaccine Delivery. *ACS Nano* **2017**, acsnano.6b07343.

[57] Nguyen, D. N.; Green, J. J.; Chan, J. M.; Langer, R.; Anderson, D. G. Polymeric Materials for Gene Delivery and DNA Vaccination. *Adv. Mater.* **2009**, *21*, 847–

867.

[58] Uto, T.; Akagi, T.; Yoshinaga, K.; Toyama, M.; Akashi, M.; Baba, M. The Induction of Innate and Adaptive Immunity by Biodegradable Poly(γ-Glutamic Acid) Nanoparticles via a TLR4 and MyD88 Signaling Pathway. *Biomaterials* **2011**, *32*, 5206–5212.

[59] Wegmann, F.; Gartlan, K. H.; Harandi, a M.; Brinckmann, S. a; Coccia, M.; Hillson, W. R.; Kok, W. L.; Cole, S.; Ho, L. P.; Lambe, T.; *et al.* Polyethyleneimine Is a Potent Mucosal Adjuvant for Viral Glycoprotein Antigens. *Nat Biotechnol* **2012**, *30*, 883–888.

[60] Reddy, S. T.; van der Vlies, A. J.; Simeoni, E.; O'Neil, C. P.; Swartz, M. a.; Hubbell, J. a. Exploiting Lymphatic Transport and Complement Activation in Nanoparticle Vaccines. *Eur. Cells Mater.* **2007**, *14*, 103.

[61] Thomas, S. N.; van der Vlies, A. J.; O'Neil, C. P.; Reddy, S. T.; Yu, S. S.; Giorgio, T. D.; Swartz, M. A.; Hubbell, J. A. Engineering Complement Activation on Polypropylene Sulfide Vaccine Nanoparticles. *Biomaterials* **2011**, *32*, 2194–2203.

[62] Raschke, W.; Baird, S.; Ralph, P.; Nakoinz, I. Functional Macrophage Cell Lines Transformed by Abelson Leukaemia Virus. *Cell* **1978**, *15*, 261–267.

[63] ASTM International. ASTM F1903-10 Standard Practice for Testing For Biological Responses to Particles In Vitro, 2010.

[64] Komohara, Y.; Fujiwara, Y.; Ohnishi, K.; Takeya, M. Tumor-Associated Macrophages: Potential Therapeutic Targets for Anti-Cancer Therapy. *Adv. Drug Deliv. Rev.* **2016**, *99*, 180–185.

[65] Hashimoto, D.; Miller, J.; Merad, M. Dendritic Cell and Macrophage Heterogeneity In Vivo. *Immunity* **2011**, *35*, 323–335.

[66] Jin, H.; Kim, A.; Miyata, K.; Kataoka, K.; Kim, H. J.; Kim, A.; Miyata, K.; Kataoka, K. Recent Progress in Development of siRNA Delivery Vehicles for Cancer Therapy. *Adv. Drug Deliv. Rev.* **2016**, *104*, 61–77.

[67] Young, S. W. S.; Stenzel, M.; Jia-Lin, Y. Nanoparticle-siRNA: A Potential Cancer Therapy? *Crit. Rev. Oncol. Hematol.* **2016**, *98*, 159–169.

[68] Pardoll, D. M. The Blockade of Immune Checkpoints in Cancer Immunotherapy. *Nat. Rev. Cancer* **2012**, *12*, 252–264.

[69] Kim, D.-H.; Behlke, M. a; Rose, S. D.; Chang, M.-S.; Choi, S.; Rossi, J. J. Synthetic dsRNA Dicer Substrates Enhance RNAi Potency and Efficacy. *Nat. Biotechnol.* **2005**, *23*, 222–226.

[70] Nakayama, M.; Akiba, H.; Takeda, K.; Kojima, Y.; Hashiguchi, M.; Azuma, M.; Yagita, H.; Okumura, K. Tim-3 Mediates Phagocytosis of Apoptotic Cells and Cross-Presentation. *Blood* **2009**, *113*, 3821–3830.

[71] Corbett, J. C. W.; Connah, M. T.; Mattison, K. Advances in the Measurement of Protein Mobility Using Laser Doppler Electrophoresis - the Diffusion Barrier Technique. *Electrophoresis* **2011**, *32*, 1787–1794.

[72] Xu, Y.; Sung, O. K.; Li, Y.; Han, J. Autophagy Contributes to Caspase-Independent Macrophage Cell Death. *J. Biol. Chem.* **2006**, *281*, 19179–19187.

[73] Hunter, C. a; Jones, S. a. IL-6 as a Keystone Cytokine in Health and Disease. *Nat. Immunol.* **2015**, *16*, 448–457.

[74] Zhang, Q.; Lenardo, M. J.; Baltimore, D. 30 Years of NF-κB: A Blossoming of

Relevance to Human Pathobiology. *Cell* **2017**, *168*, 37–57.

[75] Ikushima, H.; Negishi, H.; Taniguchi, T. The IRF Family Transcription Factors at the Interface of Innate and Adaptive Immune Responses. *Cold Spring Harb Symp Quant Biol* **2013**, *LXXVIII*.

[76] Anderson, A. C. Tim-3: An Emerging Target in the Cancer Immunotherapy Landscape. *Cancer Immunol. Res.* **2014**, *2*, 393–398.

[77] Chiba, S.; Baghdadi, M.; Akiba, H.; Yoshiyama, H.; Kinoshita, I.; Dosaka-Akita, H.; Fujioka, Y.; Ohba, Y.; Gorman, J. V; Colgan, J. D.; *et al.* Tumor-Infiltrating DCs Suppress Nucleic Acid-Mediated Innate Immune Responses through Interactions between the Receptor TIM-3 and the Alarmin HMGB1. *Nat. Immunol.* **2012**, *13*, 832–842.

[78] Ocaña-Guzman, R.; Torre-Bouscoulet, L.; Sada-Ovalle, I. TIM-3 Regulates Distinct Functions in Macrophages. *Frontiers in Immunology*, 2016, *7*, 229.

[79] Fourcade, J.; Sun, Z.; Benallaoua, M.; Guillaume, P.; Luescher, I. F.; Sander, C.; Kirkwood, J. M.; Kuchroo, V.; Zarour, H. M. Upregulation of Tim-3 and PD-1 Expression Is Associated with Tumor Antigen–specific CD8 + T Cell Dysfunction in Melanoma Patients. *J. Exp. Med.* **2010**, *207*, 2175–2186.

[80] Sakuishi, K.; Apetoh, L.; Sullivan, J. M.; Blazar, B. R.; Kuchroo, V. K.; Anderson, A. C. Targeting Tim-3 and PD-1 Pathways to Reverse T Cell Exhaustion and Restore Anti-Tumor Immunity. *J. Exp. Med.* **2010**, *207*, 2187–2194.

[81] Sakuishi, K.; Ngiow, S. F.; Sullivan, J. M.; Teng, M. W. L.; Kuchroo, V. K.; Smyth, M. J.; Anderson, A. C. TIM3 + FOXP3 + Regulatory T Cells Are Tissue-

Specific Promoters of T-Cell Dysfunction in Cancer. *Oncoimmunology* **2013**, *2*, e23849.

[82] Passwell, J. H.; Steward, M. W.; Soothill, J. F. Inter-Mouse Strain Differences in Macrophage Function and Its Relationship to Antibody Responses. *Clin. Exp. Immunol.* **1974**, *17*, 159–167.

[83] Sellers, R. S.; Clifford, C. B.; Treuting, P. M.; Brayton, C. Immunological Variation Between Inbred Laboratory Mouse Strains: Points to Consider in Phenotyping Genetically Immunomodified Mice. *Vet. Pathol.* **2012**, *49*, 32–43.

[84] Mangraviti, A.; Tzeng, S. Y.; Kozielski, K. L.; Wang, Y.; Jin, Y.; Gullotti, D.; Pedone, M.; Buaron, N.; Liu, A.; Wilson, D. R.; *et al.* Polymeric Nanoparticles for Nonviral Gene Therapy Extend Brain Tumor Survival in Vivo. *ACS Nano* **2015**, *9*, 1236–1249.

[85] Afonina, I. S.; Zhong, Z.; Karin, M.; Beyaert, R. Limiting Inflammation—the Negative Regulation of NF-κB and the NLRP3 Inflammasome. *Nat. Immunol.* **2017**, *18*, 861–869.

[86] Muñoz-Planillo, R.; Kuffa, P.; Martínez-Colón, G.; Smith, B. L.; Rajendiran, T. M.; Núñez, G. K+ Efflux Is the Common Trigger of NLRP3 Inflammasome Activation by Bacterial Toxins and Particulate Matter. *Immunity* **2013**, *38*, 1142–1153.

[87] Hawley, K. L.; Olson, C. M.; Iglesias-Pedraz, J. M.; Navasa, N.; Cervantes, J. L.; Caimano, M. J.; Izadi, H.; Ingalls, R. R.; Pal, U.; Salazar, J. C.; *et al.* CD14 Cooperates with Complement Receptor 3 to Mediate MyD88-Independent Phagocytosis of Borrelia Burgdorferi. *Proc. Natl. Acad. Sci. U. S. A.* **2012**, *109*,

1228–1232.

[88] Mestas, J.; Hughes, C. C. W. Of Mice and Not Men: Differences between Mouse and Human Immunology. *J. Immunol.* **2004**, *172*, 2731–2738.

[89] Waring, M. J.; Arrowsmith, J.; Leach, A. R.; Leeson, P. D.; Mandrell, S.; Owen, R. M.; Pairaudeau, G.; Pennie, W. D.; Pickett, S. D.; Wang, J.; *et al.* An Analysis of the Attrition of Drug Candidates from Four Major Pharmaceutical Companies. *Nat. Rev. Drug Discov.* **2015**, *14*, 475–486.

[90] Thomas, D. W.; Burns, J.; Audette, J.; Caroll, A.; Dow-Hygelund, C.; Hay, M. *Clinical Development Success Rates 2006-2015*; 2016.

[91] Lupetti, R.; Pisarra, P.; Verrecchia, A.; Farina, C.; Nicolini, G.; Anichini, A.; Bordignon, C.; Sensi, M.; Parmiani, G.; Traversari, C. Translation of a Retained Intron in Tyrosinase-Related Protein (TRP) 2 mRNA Generates a New Cytotoxic T Lymphocyte (CTL)-Defined and Shared Human Melanoma Antigen Not Expressed in Normal Cells of the Melanocytic Lineage. *J. Exp. Med.* **1998**, *188*, 1005–1016.

[92] Iribarren, K.; Bloy, N.; Buqué, A.; Cremer, I.; Eggermont, A.; Fridman, W. H.; Fucikova, J.; Galon, J.; Špíšek, R.; Zitvogel, L.; *et al.* Trial Watch: Immunostimulation with Toll-like Receptor Agonists in Cancer Therapy. *Oncoimmunology* **2016**, *5*, e1088631.

[93] Afonin, K. A.; Bindewald, E.; Yaghoubian, A. J.; Voss, N.; Jacovetty, E.; Shapiro, B. A.; Jaeger, L. In Vitro Assembly of Cubic RNA-Based Scaffolds Designed in Silico. *Nat. Nanotechnol.* **2010**, *5*, 676–682.

[94] Afonin, K. A.; Viard, M.; Koyfman, A. Y.; Martins, A. N.; Kasprzak, W. K.;

Panigaj, M.; Desai, R.; Santhanam, A.; Grabow, W. W.; Jaeger, L.; *et al.* Multifunctional RNA Nanoparticles. *Nano Lett.* **2014**, *14*, 5662–5671.

[95] Afonin, K. A.; Viard, M.; Kagiampakis, I.; Case, C. L.; Dobrovolskaia, M. A.; Hofmann, J.; Vrzak, A.; Kireeva, M.; Kasprzak, W. K.; KewalRamani, V. N.; *et al.* Triggering of RNA Interference with RNA–RNA, RNA–DNA, and DNA–RNA Nanoparticles. *ACS Nano* **2015**, *9*, 251–259.

[96] Afonin, K. a; Grabow, W. W.; Walker, F. M.; Bindewald, E.; Dobrovolskaia, M. a; Shapiro, B. a; Jaeger, L. Design and Self-Assembly of siRNA-Functionalized RNA Nanoparticles for Use in Automated Nanomedicine. *Nat. Protoc.* **2011**, *6*, 2022–2034.

[97] Halman, J. R.; Satterwhite, E.; Roark, B.; Chandler, M.; Viard, M.; Ivanina, A.; Bindewald, E.; Kasprzak, W. K.; Panigaj, M.; Bui, M. N.; *et al.* Functionally-Interdependent Shape-Switching Nanoparticles with Controllable Properties. *Nucleic Acids Res.* **2017**, *5*, gkx008.

[98] Johansen, P.; Storni, T.; Rettig, L.; Qiu, Z.; Der-Sarkissian, A.; Smith, K. A.; Manolova, V.; Lang, K. S.; Senti, G.; Müllhaupt, B.; *et al.* Antigen Kinetics Determines Immune Reactivity. *Proc. Natl. Acad. Sci. U. S. A.* **2008**, *105*, 5189–5194.

[99] Jewell, C. M.; Bustamante Lopez, S. C.; Irvine, D. J. In Situ Engineering of the Lymph Node Microenvironment via Intranodal Injection of Adjuvant-Releasing Polymer Particles. *Proc. Natl. Acad. Sci.* **2011**, *108*, 15745–15750.

[100] Afonin, K. A.; Kasprzak, W.; Bindewald, E.; Puppala, P. S.; Diehl, A. R.; Hall, K. T.; Kim, T. J.; Zimmermann, M. T.; Jernigan, R. L.; Jaeger, L.; *et al.*

Computational and Experimental Characterization of RNA Cubic Nanoscaffolds. *Methods* **2014**, *67*, 256–265.

[101] Afonin, K. A.; Kireeva, M.; Grabow, W. W.; Kashlev, M.; Jaeger, L.; Shapiro, B. A. Co-Transcriptional Assembly of Chemically Modified RNA Nanoparticles Functionalized with siRNAs. *Nano Lett.* **2012**, *12*, 5192–5195.

[102] Parlea, L.; Puri, A.; Kasprzak, W.; Bindewald, E.; Zakrevsky, P.; Satterwhite, E.; Joseph, K.; Afonin, K. A.; Shapiro, B. A. Cellular Delivery of RNA Nanoparticles. *ACS Comb. Sci.* **2016**, *18*, 527–547.

[103] Singh, V.; Ji, Q.; Feigenbaum, L.; Leighty, R. M.; Hurwitz, A. A. Melanoma Progression Despite Infiltration by In Vivo-Primed TRP-2–specific T Cells. *J. Immunother.* **2009**, *32*, 129–139.

[104] Overwijk, W. W.; Tsung, A.; Irvine, K. R.; Parkhurst, M. R.; Goletz, T. J.; Tsung, K.; Carroll, M. W.; Liu, C.; Moss, B.; Rosenberg, S. a; *et al.* gp100/pmel 17 Is a Murine Tumor Rejection Antigen: Induction Of "self"-Reactive, Tumoricidal T Cells Using High-Affinity, Altered Peptide Ligand. *J. Exp. Med.* **1998**, *188*, 277–286.

[105] Wei, F.; Yang, D.; Tewary, P.; Li, Y.; Li, S.; Chen, X.; Howard, O. M. Z.; Bustin, M.; Oppenheim, J. J. The Alarmin HMGN1 Contributes to Antitumor Immunity and Is a Potent Immunoadjuvant. *Cancer Res.* **2014**, *74*, 5989–5998.

[106] Thomas, S. N.; Vokali, E.; Lund, A. W.; Hubbell, J. A.; Swartz, M. A. Targeting the Tumor-Draining Lymph Node with Adjuvanted Nanoparticles Reshapes the Anti-Tumor Immune Response. *Biomaterials* **2014**, *35*, 814–824.

[107] Kourtis, I. C.; Hirosue, S.; de Titta, A.; Kontos, S.; Stegmann, T.; Hubbell, J. A.;

Swartz, M. A. Peripherally Administered Nanoparticles Target Monocytic Myeloid Cells, Secondary Lymphoid Organs and Tumors in Mice. *PLoS One* **2013**, *8*, e61646.

[108] Tschuch, C.; Schulz, A.; Pscherer, A.; Werft, W.; Benner, A.; Hotz-Wagenblatt, A.; Barrionuevo, L. S.; Lichter, P.; Mertens, D. Off-Target Effects of siRNA Specific for GFP. *BMC Mol. Biol.* **2008**, *9*, 60.

[109] Ho, P. P.; Fontoura, P.; Ruiz, P. J.; Steinman, L.; Garren, H. An Immunomodulatory GpG Oligonucleotide for the Treatment of Autoimmunity via the Innate and Adaptive Immune Systems. *J. Immunol.* **2003**, *171*, 4920–4926.